



HAL
open science

Car sickness in real driving conditions: Effect of lateral acceleration and predictability reflected by physiological changes

Eléonore Henry, Clément Bougard, Christophe Bourdin, Lionel Bringoux

► To cite this version:

Eléonore Henry, Clément Bougard, Christophe Bourdin, Lionel Bringoux. Car sickness in real driving conditions: Effect of lateral acceleration and predictability reflected by physiological changes. *Transportation Research Part F: Traffic Psychology and Behaviour*, 2023, 97, pp.123-139. 10.1016/j.trf.2023.06.018 . hal-04397386

HAL Id: hal-04397386

<https://hal.science/hal-04397386>

Submitted on 17 Jan 2024

HAL is a multi-disciplinary open access archive for the deposit and dissemination of scientific research documents, whether they are published or not. The documents may come from teaching and research institutions in France or abroad, or from public or private research centers.

L'archive ouverte pluridisciplinaire **HAL**, est destinée au dépôt et à la diffusion de documents scientifiques de niveau recherche, publiés ou non, émanant des établissements d'enseignement et de recherche français ou étrangers, des laboratoires publics ou privés.

1
2
3
4
5
6
7
8
9
10
11
12
13
14
15
16
17
18
19
20
21
22
23
24
25
26
27
28
29
30
31
32

Car sickness in real driving conditions : Effect of lateral acceleration and predictability reflected by physiological changes

Eléonore Henry^{1,2}, Clément Bougard^{1,2}, Christophe Bourdin², Lionel Bringoux²

¹ *Stellantis, Centre Technique de Vélizy, Vélizy-Villacoublay, France*

² *Aix Marseille Univ, CNRS, ISM, Marseille, France*

Corresponding author :

Eléonore HENRY
163, av. de Luminy F
13288 Marseille cedex 09 (France)

E-mail address:

eleonorehenry96@gmail.com
clement.bougard@stellantis.com
christophe.bourdin@univ-amu.fr
lionel.bringoux@univ-amu.fr

Declarations of interest: none.

33 **Abstract**

34 With the development of autonomous vehicles, car sickness may affect increasing numbers of car
35 occupants. Car manufacturers have a real need to understand the causes of these symptoms, which
36 occur mainly when car occupants are not engaged in a driving task. This study is the first to
37 evaluate, in real driving conditions, the impact of lateral acceleration level and vehicle path
38 predictability on car sickness incidence and severity, and the potential relationship with
39 physiological changes. 24 healthy volunteers participated as front seat passengers in a slalom
40 session inducing lateral movements at very low frequency (0.2 Hz). They were continuously
41 monitored via physiological recordings and provided subjective car sickness ratings (CSR) after
42 each slalom, using a 5-point likert scale. CSR reveal that (i) the greater the lateral acceleration and
43 (ii) the less predictable the vehicle path, the more severe the car sickness symptoms in real driving
44 conditions. An increase in several physiological parameters is also found simultaneously with
45 higher CSR, demonstrating activation of the sympathetic nervous system. Moreover, the linear
46 regression applied to our data suggests that these physiological parameters can be used to indicate
47 car sickness severity. Moreover, the linear regression applied to our data suggests that the
48 evolution of these physiological parameters may reflect the CSR level indicated by participants.
49

50 **Keywords:** Lateral acceleration, predictability, physiological measures, car sickness, real driving

51
52
53
54
55
56
57
58
59
60
61
62
63
64
65
66

67 1 Introduction

68 Car sickness is very common, affecting about 60% of the population (Diels, 2014), mainly
69 passengers, half of whom present high susceptibility and severe symptoms (Rolnick & Lubow,
70 1991; Chen et al., 2010; Bos et al., 2018). Indeed, exposure to certain car motion can lead to car
71 sickness symptoms ranging from mild stomach aches or headaches to dizziness, nausea, and
72 ultimately vomiting (Dennison et al., 2016; Green, 2016). However, the development of
73 autonomous vehicles, turning drivers into passengers (Sivak & Schoettle, 2015; Diels & Bos,
74 2016; Kuiper, Bos, Diels, et al., 2020a), should sharply increase the numbers exposed to car
75 sickness (Diels, 2014; Kuiper et al., 2018). This would run counter to the promise of enhanced
76 driver comfort during transport (Diels & Bos, 2016; Salter et al., 2019). Thus, understanding what
77 induces these symptoms is currently a major concern for car manufacturers, particularly when the
78 car occupant is not engaged in a driving task.

79 Studies with this objective have so far been mainly conducted in laboratories, rarely in real
80 vehicles. However, it was demonstrated that the sensory context induced by laboratory stimuli will
81 always diverge from that in a real car (Mühlbacher et al., 2020). For example, when a rotating
82 chair is used, the stimuli are mainly force-related, inducing vestibular and somatosensory
83 solicitations which may cause some motion sickness (eg. coriolis or somatogyral illusions
84 (Lackner, 2014)). Conversely, with a virtual reality headset, the stimuli are only visual, leading to
85 visually-induced motion sickness (VIMS) (Naqvi et al., 2015; Dennison et al., 2016; Kim & Park,
86 2020). Some attempts have been made to create a more realistic driving environment using
87 dynamic driving simulators (combination of virtual reality + physical motion) (Lin et al., 2007;
88 Chen et al., 2010; Aykent et al., 2014). While this has the advantage of engaging multimodal
89 sensory inputs, the latter can never precisely replicate cars' movements (Mühlbacher et al., 2020).
90 Therefore, no consensus on the exact origins of car sickness has been reached, principally due to
91 the diversity of conditions and stimuli used in these studies.

92 Studies on motion sickness tend to focus first on the vertical movements very common in
93 situations inducing sea sickness and air sickness. The characteristics of the motion itself (e.g.
94 acceleration, frequency, duration, speed, axis, etc.) are known to influence the occurrence and
95 severity of motion sickness (Lawther & Griffin, 1987; Bos & Bles, 1998; Koohestani et al., 2019).
96 Movements at very low frequency induce symptoms, especially when oscillating between 0.10
97 and 0.50 Hz (Turner, 1999; Golding et al., 2001; Donohew & Griffin, 2004; Cheung & Nakashima,
98 2006). In laboratory conditions investigating vertical movements, pioneering modeling work
99 identified a critical threshold between 0.16 and 0.20 Hz inducing the highest incidence of motion
100 sickness (O'Hanlon & McCauley, 1974). Since inertial forces tend to be interpreted by the
101 vestibular system as translational above 0.20 Hz and as tilt below this value, such a frequency
102 should be sufficient to create strong intravestibular conflict (Bos & Bles, 1998). In addition,
103 Lawther and Griffin (1987) found a linear relationship between the magnitude of vertical
104 accelerations on ships and the incidence of motion sickness (MSI). With a range of 0.0 to 5.4 m/s²,

105 an adapted McCauley's (1974) model showed a sigmoidal relationship between vertical
106 acceleration magnitude and MSI: the greater the vertical acceleration, the more rapid the onset and
107 the more severe the symptoms (O'Hanlon & McCauley, 1974; Bos & Bles, 1998). In cars,
108 however, horizontal accelerations caused by braking (longitudinal) and turning (lateral) were
109 shown to play a greater role in sickness incidence than vertical accelerations (Cheung &
110 Nakashima, 2006; Diels, 2014). A recent systematic review (Schmidt et al., 2020) found that the
111 triggers of car sickness most frequently cited were those involving repeated lateral acceleration
112 (multiple turns [71.8%], winding roads [70.5%]). It is actually lateral motion at very low
113 frequency, around 0.2 Hz, that was found to be the principal component of car sickness (Wada &
114 Yoshida, 2016; Kuiper et al., 2018; Henry et al., 2022). Strikingly however, no study so far has
115 specifically investigated the impact of different levels of lateral acceleration on car sickness
116 severity in real driving conditions.

117 For car manufacturers, there is another key issue: the difference in passengers' and drivers'
118 susceptibility to car sickness. This difference mainly arises from the driver's ability to control and
119 anticipate vehicle paths (Griffin & Newman, 2004; Perrin et al., 2013; Wada & Yoshida, 2016).
120 Conversely, passengers are passively exposed to vehicle motion and have a limited knowledge of
121 forthcoming actions (e.g., direction, speed, strength, duration etc.). Several studies conclude that
122 the ability to predict future movements may reduce the level of motion sickness induced (Rolnick
123 & Lubow, 1991; Feenstra et al., 2011; Levine et al., 2014). These observations are supported by
124 the theory of sensory mismatch, which occurs when perceptual expectations from the internal
125 model about upcoming sensory inputs do not match those actually perceived (Reason, 1978;
126 Dennison et al., 2016). In other words, passengers may experience discrepancies between their
127 expectations and reality, whereas drivers planning their driving control actions can precisely
128 anticipate vehicle motion (Griffin & Newman, 2004; Perrin et al., 2013; Wada et al., 2018). In
129 addition, the magnitude of this discrepancy seems to impact the symptom severity of motion
130 sickness (Dennison et al., 2016; Kuiper, Bos, Schmidt, et al., 2020b). While sensory mismatch is
131 often suggested as a cause of car sickness, however, less is known about how vehicle path
132 unpredictability may affect car sickness severity in real driving conditions.

133 Accurate analysis of the impact of each factor inducing motion sickness requires a method of
134 identifying and assessing the symptoms. Currently, the most widely used are questionnaires
135 (MSSQ (Golding, 2006); MSAQ (Gianaros et al., 2003); SSQ (Kennedy, 1993) etc.) and subjective
136 scales (MISC (Bos et al., 2006); Griffin and Newman's scale, (2004) etc.). However, both depend
137 on the individual's subjective feelings and on how the individual interprets the scale in reporting
138 discomfort. Moreover, both tools suffer from low temporal and sickness resolution (Irmak, 2021).
139 There is clearly a need for a more reliable and objective method of measuring motion sickness
140 severity.

141 Given the nature of the symptoms observed, physiological indicators could be a promising
142 complement. In fact, motion sickness is considered a neuro-vegetative crisis that can initiate

143 physiological changes, also commonly observed during stressful events (Money, 1970; Gianaros
144 et al., 2003; Muth, 2006). Attempts have been made to identify these changes for an objective
145 measure of motion sickness, by exploring several physiological variables: electrocardiography
146 (ECG), respiration (RSP), electrodermal activity (EDA), electrogastrogram (EGG), and
147 electroencephalography (EEG). Multiple features have been extracted from each variable, most
148 commonly: heart rate (HR) and heart rate variability (HRV) for ECG, breathing rate (BR) for RSP,
149 mean skin conductance level (SCL) and response (SCR) for EDA, stomach contraction activity for
150 EGG, and changes in frequency band content for EEG (Kim et al., 2005; Dahlman et al., 2009;
151 Dennison et al., 2016; Koohestani et al., 2019; Henry et al., 2022). However, although most of the
152 motion sickness studies were conducted in laboratory environments, their results were not
153 consistent, possibly due to the wide variety of devices and stimuli used (Koohestani et al., 2019).
154 For example, when measuring HR, some studies reported a decrease using a rotating optokinetic
155 drum (Hu et al., 1991) and VIMS (VR (Nalivaiko et al., 2015; Dennison et al., 2016); Static driving
156 simulator (Kim et al., 2005)), while others found an increase in HR with similar devices but
157 different stimuli (rotating optokinetic drum (Dahlman et al., 2009); VR (Cheung, 2004; Himi et
158 al., 2004)). Between-study discrepancies in results were also observed for HRV, BR, and EDA
159 measurements (Hu et al., 1991; Kim et al., 2005; Dahlman et al., 2009; LaCount et al., 2009;
160 Nalivaiko et al., 2015; Dennison et al., 2016; Gavvani et al., 2017; Islam et al., 2020). Where car
161 sickness symptoms are evaluated in real driving conditions, only one study measures physiological
162 variables (Irmak, 2021), with results indicating a clear link between EDA features and symptom
163 severity, as well as a slight increase in HR. It has been suggested that depending on the
164 environments, stimuli, and induced movements, the nervous system may be stimulated to a
165 variable degree (Harm, 2002). This could explain the divergence in physiological responses and
166 the lack of consensus on the indicators that can be considered predictive of motion sickness.

167 Individual reactions to motion thus vary in intensity and complexity with the movements to
168 which participants are exposed. Seeking a more realistic assessment than that provided by
169 laboratory conditions, this study was conducted in real car driving conditions using 0.2 Hz lateral
170 movements. Our aim was to assess how (i) lateral acceleration level and (ii) ability to predict
171 vehicle path impacted the severity of passengers' car sickness. Based on the literature, we
172 hypothesized that (i) the stronger the acceleration, the more severe the symptoms and (ii) inability
173 to predict vehicle path also exacerbates symptoms in real driving conditions. Another major
174 objective was to relate possible physiological responses to car sickness and to determine which
175 variables might indicate car sickness severity in real driving conditions. We hypothesized that (i)
176 the parameters of interest for each measure (cardiac, respiratory, and electrodermal) would
177 increase gradually throughout the stimulation, reflecting the activation of the sympathetic nervous
178 system, (ii) each of these parameters would be impacted during the post-test period, and (iii) their
179 respective evolution should be linked to increasing symptom severity.

180

181 **2 Materials and methods**

182 **2.1 Participants**

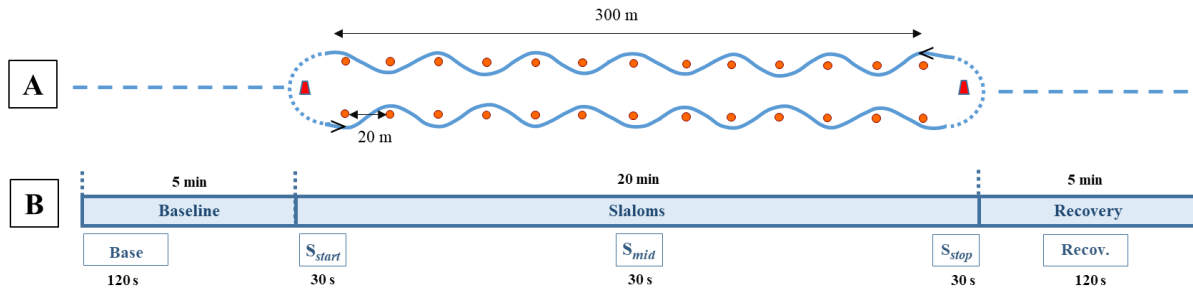
183 Twenty-four healthy right-handed volunteers (12 women and 12 men, mean age: 39.3 ± 9
184 years) with no neurological or vestibular disorders took part in the experiment, having drunk no
185 stimulating or alcoholic drinks in the previous 24 hours. Minimum age was 20 years, with a
186 driver's license held for at least 2 years. As mentioned in the introduction, autonomous vehicles,
187 by turning drivers into passengers, are likely to expose them to car sickness. Given that half the
188 passengers affected by car sickness show high susceptibility, we therefore focused on this
189 population (Bos et al., 2018). To guarantee sample homogeneity and limit inter-individual
190 variability, participants were selected for their high susceptibility to motion sickness and car
191 sickness, assessed by the Motion Sickness Susceptibility Questionnaire (mean percentile score:
192 $90.6 \pm 9.2\%$ (Golding, 2006)). Participants were informed of the study procedure and general
193 objectives before signing a consent form warning them that they might experience car sickness
194 during test sessions and that they could withdraw from the experiment at any time and for any
195 reason. One participant became too sick to finish the experiment and quit the study. Participation
196 was unpaid and no conflict of interest was declared. This study was approved by the local ethics
197 committee of Aix-Marseille University in accordance with the ethical standards laid down in the
198 1964 Declaration of Helsinki.

199 **2.2 General experimental set-up**

200 Test sessions were conducted in a closed area approximately 400 m long and 50 m wide, with
201 no other traffic present, for controllability and safety reasons. The vehicle used for these tests was
202 a medium-sized car popular in France (Citroën C4 Picasso), driven by one professional driver
203 specifically trained to produce reproducible vehicle dynamics for all participants. During the test
204 session, participants were seated in the front passenger seat of the vehicle in a predefined sitting
205 position, safety belt fastened. We focused on the front passenger position to replicate as closely as
206 possible what happens when a driver becomes a passenger (in autonomous vehicles), mainly in
207 terms of the visual and vestibular experience. Car ventilation and temperature were monitored to
208 provide a similar controlled environment for each participant. They were continuously equipped
209 with physiological modules for electrocardiogram (ECG), respiration (RSP), and electrodermal
210 activity (EDA) recordings (detailed further). A slider was positioned in front of volunteers to allow
211 them to indicate their car sickness level during every test period (equipment detailed below). For
212 synchronization, data from the physiological modules, the car sickness rating slider, and the
213 vehicle's Controller Area Network (CAN) were recorded by a laptop in the rear seat of the vehicle.
214 The experimental road consisted of two straight segments approximately 300 m long with 10m-
215 radius turning zones at both ends, forming an oval track. Three rows of twelve pylons spaced 20m
216 apart were located along both straight segments, with a 6m gap between rows (Fig 1 - A).

217 **2.3 Procedure**

218 Every test session began with one baseline period of 5 min in the parked car, during which
 219 resting physiological recordings were collected and signal quality was assessed visually (online
 220 check). Next came a slalom period of about 20 min to induce car sickness symptoms. If participants
 221 felt too sick to finish the test (i.e., maximum rating of 4 on the discomfort scale), the slalom period
 222 was interrupted, and the vehicle was parked. Once the vehicle stopped, there was a static recovery
 223 period of 5 min. During all periods, participants were instructed to look frontwards and to move
 224 as little as possible. Each participant took part in two test sessions on the same day, with a one-
 225 hour lag between sessions, which lasted approximately 60 minutes (participant equipment, testing,
 226 and debriefing). At the end of their second test session, participants were given details of the
 227 study’s objectives and thanked for volunteering.

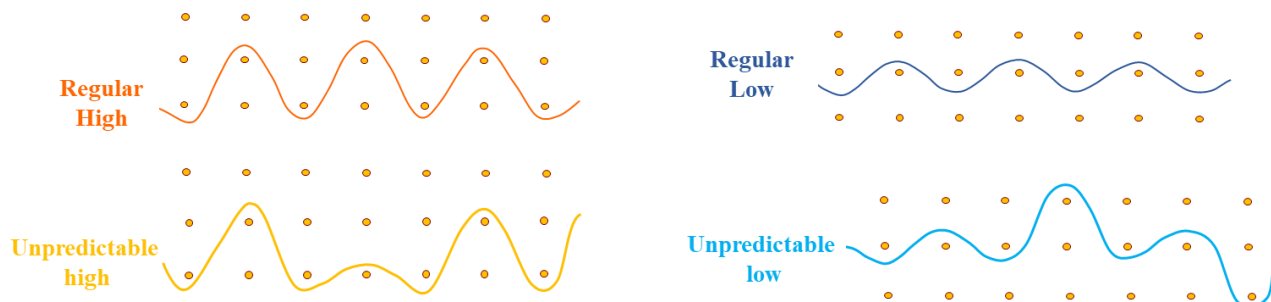


228 **Figure 1:** Representation of (A) test set-up and timeline of the test session, in periods: baseline, slalom, recovery; (B)
 229 the five time intervals per session analyzed: baseline (Base), slaloms (comprising S_{start} , S_{mid} , S_{stop}), and recovery (Recov).
 230 See Section 4 Data acquisition and processing.
 231

232 During the slalom period, the car was driven at a continuous speed of about 35 km/h and, in
 233 order to minimize additional lateral acceleration, the speed was limited to about 15 km/h during
 234 U-turns. The gap between pylons and the car speed ensured lateral movements of close to 0.2 Hz,
 235 recognized as a car-sickness-inducing frequency (Bos & Bles, 1998).

236 Four conditions were designed to examine the effects of two independent variables. Two
 237 conditions assessed the influence of degree of lateral acceleration in regular slaloms, while two
 238 others assessed the influence of inability to predict vehicle path in both regular and unpredictable
 239 slaloms. The purely regular slalom conditions involved two levels of acceleration: high (5 m.s^2)
 240 called Regular High (RH) and low (2 m.s^2) called Regular Low (RL) (Fig 2 – A). These
 241 acceleration levels were based on the McCauley (1974) vertical model: low acceleration (2 m/s^2)
 242 causing 50% of MSI and the model’s highest acceleration (5 m/s^2) causing maximum MSI
 243 (O’Hanlon & McCauley, 1974; Bos & Bles, 1998). During each regular slalom, the driver
 244 executed zigzags to the left and right of the pylons to induce reproducible lateral acceleration
 245 levels. In the unpredictable slalom conditions, the vehicle followed the path of a regular slalom
 246 but, at a given time, the driver added an unpredictable turn in an unexpected way. When the regular
 247 slalom path acceleration was high, the unpredictable turn was performed at low acceleration: this

248 is termed the Unpredictable High (UH) condition. In conditions with low regular slalom path
249 acceleration, the unpredictable turn was performed at high acceleration: the Unpredictable Low
250 (UL) condition (Fig 2 – B). Each participant took part in both a regular and an unpredictable
251 condition at the same acceleration level.



252
253 **Figure 2:** Representations of the four experimental conditions assessing the influence of lateral acceleration (High vs
254 Low conditions) and inability to predict vehicle path (Regular vs Unpredictable conditions).

255 2.4 Data acquisition

256 2.4.1 CAN recordings

257 The vehicle’s CAN data were recorded to obtain speed, lateral acceleration, and frequency of
258 movement oscillations. Sampling frequency was set at 100 Hz. Each slalom (start and end) was
259 automatically identified from the level of lateral acceleration, using MATLAB software
260 (MathWorks, 2017).

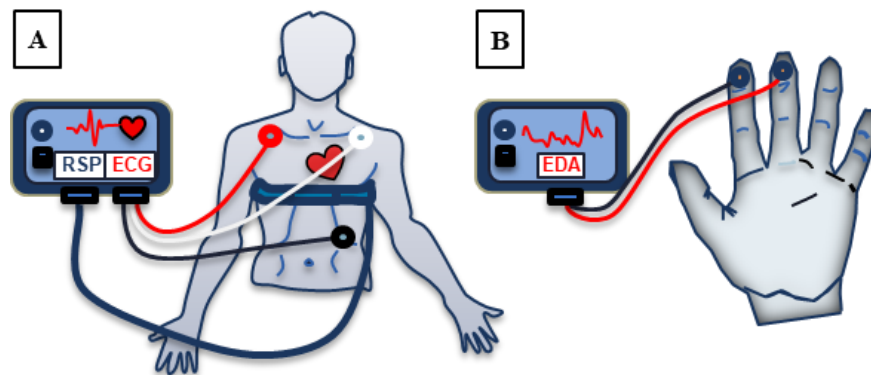
261 2.4.2 Car sickness rating recordings

262 The test included regular subjective assessments of car sickness severity, used to analyze the
263 evolution of symptoms from their very first occurrence and to compare it with the evolution of
264 physiological recordings. To limit the time spent scoring, we therefore chose a short and
265 continuous scale using a slider, which was easy to understand and to remember. Based on the first
266 five levels of Griffin and Newman’s scale (2004), a 5-point likert scale was defined, graduated
267 from 0 to 4: 0 = No symptom, 1 = Any symptom, however slight, 2 = Mild symptoms, for example,
268 stomach awareness but no nausea, 3 = Mild nausea, 4 = Mild to moderate nausea (Green, 2016;
269 Wada & Yoshida, 2016). The field was divided into 4 equal segments only indicated by colored
270 dots, so that the participants were guided in evaluating their discomfort without being influenced
271 by numbers. Each color corresponded to a rating: green for 0, white for 1 and 2, orange for 3 and
272 red for 4. Participants rated their car sickness level via the slider in front of them. Only one score
273 was recorded for baseline and one for the recovery period. In the slalom period, during the U-turns
274 that followed each slalom, participants were instructed to give their rating based on the worst
275 symptoms they experienced in the slalom just completed. Thus, since a slalom lasted about 30 sec,
276 a score was obtained every 30 sec during the slalom period. One advantage of this method lies in

277 its immediate assessment of car sickness symptoms, without test interruption and with attention
278 only diverted for a few seconds during U-turns (periods not analyzed).

279 2.4.3 Physiological recordings

280 Participants were continuously monitored to record physiological measurements with
281 Bionomadix devices connected to a BIOPAC MP160 (BIOPAC Systems, Inc.). Physiological
282 signals were amplified and recorded at a sample rate of 1000 Hz. Following a classical
283 configuration, ECG was recorded with three disposable, pre-gelled Ag/AgCl 11mm surface
284 electrodes (EL503, BIOPAC Systems, Inc.) located on the left and right collarbone and in the 7th
285 intercostal space. EDA was detected using two disposable, pre-gelled Ag/AgCl 11mm electrodes
286 (EL507, BIOPAC Systems, Inc.) placed on the index and middle finger of the non-dominant hand.
287 This electrode location was chosen with a view to participants' comfort; moreover, several studies
288 previously reported significant correlations between skin conductance recorded at the palmar
289 finger site and motion sickness severity (Hu et al., 1991; Kim et al., 2005; LaCount et al., 2011;
290 Sclocco et al., 2016; Irmak, 2021). RSP was recorded by a sensor band wrapped around the
291 participant's chest (Fig 3).



292

293 **Figure 3:** Configuration of physiological measurement. (A) ECG and respiration belt measures: electrode
294 configuration (white = VIN+, black = VIN-, red= ground) and position to obtain ECG. (B) EDA measures: electrode
295 placement used to obtain EDA signals. The ground electrode (black) was placed on the middle finger and the active
296 electrode (red) on the index finger on each participant's non-dominant hand. Leads (115 Series, BIOPAC Systems,
297 Inc.) with light-weight pinch clips connected to thin wires were attached to all electrodes and plugged into wireless
298 transmitters adhering to the chest (ECG, respiration belt) or wrist (EDA) of the participant.

299 2.5 Physiological data processing

300 For data processing, six different phases of recordings common to all participants were selected
301 for further analyses [(1) baseline (Base- first 120 s), (2) the first slalom (S_{start} - 30s), (3) the middle
302 slalom (S_{mid} - 30s), (4) the last slalom (S_{stop} - 30s), (5) the highest-CSR slalom (S_{max} - 30s), and
303 (6) recovery (Recov - middle 120 s) (Fig. 1 - B)]. Reference measurements were obtained from
304 the baseline period. One car sickness rating was obtained for each slalom and each was linked to

305 corresponding physiological recordings. For each participant, S_{\max} was the highest car sickness
306 level reported, as suggested by Chen et al. (2010) and Keshavarz et al. (2022). Finally, post-
307 stimulation reactions were assessed via a rating recorded after 120s of recovery.

308 Recording physiological parameters under ecological conditions is a technological challenge.
309 A method of pre-processing and physiological feature extraction therefore had to be developed
310 and adapted to our data, which contained more artifacts than average because of noise induced by
311 the vehicle's and the participants' movements. This required several operations to obtain clean and
312 useful signals. In addition, for the sake of clarity, only relevant physiological features were used.
313 Our method involved the following steps.

314 2.5.1 Pre processing

315 Physiological raw signals were pre-processed on the selected periods of interest (Base, S_{start} ,
316 S_{mid} , S_{max} , S_{stop} , and Recov) (Fig. 1 - B). As physiological signals are time series, it is common to
317 use wavelets to decompose them into frequency and time-frequency representations, with the
318 wavelet coefficients chosen as characteristics (Shoeb & Clifford, 2005; Li & Chung, 2013;
319 Pukhova et al., 2017). An advantage of wavelet features is their ability to encode a time and
320 frequency resolution trade-off allowing signal responses to car sickness to be captured in different
321 time windows. More specifically, we used soft and Daubechies 4 tap (Db4) wavelets obtained
322 respectively from discontinuous and continuous base functions (Mother Wavelet: db4; Mode: Soft;
323 Method: Sure Shrink; Level: 5). The chosen SureShrink method is an automatic procedure that,
324 from decomposition coefficients at level 5, minimizes the unbiased estimate of mean square error.
325 Once this step was completed, each physiological signal was filtered and cleaned using artifact
326 removal techniques. Our method for ECG signals involved unsupervised artifact detection using
327 an Isolation Forest model applied to 5-second signal intervals. Any abnormal intervals detected
328 were replaced with the closest clean segment of the signal. To avoid overlap between the replaced
329 signal and the PQRST waves in the previous and subsequent intervals, we applied two rules: i) if
330 the interval between the two R waves was less than 600ms, one of the waves was removed; ii) if
331 the interval between the two R waves was greater than 1100ms, a new R wave was inserted
332 between them (Salahuddin et al., 2007; Nunan et al., 2010). Furthermore, we used the Python
333 NeuroKit library (Carreiras et al., 2015; Makowski, 2016) to apply two classical filtering methods
334 addressing baseline slow drift and power line interference. More precisely, each ECG signal
335 underwent 50 Hz power-line noise-filtering that involved smoothing the signal with a moving
336 average kernel having a one-period width of 50 Hz. In addition, a Butterworth high pass filter with
337 a cut-off frequency of 0.5Hz was applied to remove baseline slow drifts. To process the respiratory
338 signal, we applied a classical filtering technique using Python NeuroKit library (Carreiras et al.,
339 2015; Makowski, 2016). A Butterworth band-pass filter with a low-cut frequency of 0.05Hz and a
340 high-cut frequency of 0.35Hz was used to remove baseline drift and high frequency noise from the
341 respiratory signal. Concerning EDA signals, supervised artifact removal was performed via an
342 SVM-based model (Taylor et al., 2015). The binary model was already trained on a dataset of 5-

343 second EDA signals labeled ‘normal’ or ‘abnormal’ (Taylor et al., 2015). We used this model on
344 our EDA samples, replacing the artifacts by the mean of the current 5-second signal. In addition,
345 any remaining artifacts were dealt with by a second removal applied to each 1-second signal
346 interval via a second derivative model. Finally, the EDA signal underwent Butterworth low pass
347 filtering at 3Hz using Python NeuroKit library (Carreiras et al., 2015; Makowski, 2016).

348 2.5.2 Feature extraction

349 Once signals were pre-processed, physiological features were calculated from ECG, RSP, and
350 EDA signals, using Python software (Python Software Foundation) with BioSPPy and NeuroKit
351 libraries (Carreiras et al., 2015; Makowski, 2016). Features were computed for all signals on every
352 30-second window without overlapping. Key to ECG signal processing is analyzing and
353 understanding the QRS complex waveform representing the ventricular depolarization (Yan et al.,
354 2003). A QRS detection algorithm was used to extract ECG features using the BioSPPy library.
355 We selected from the analyses performed slalom by slalom (30s) the features mean heart rate
356 (‘Hr_mean’) and standard deviation of heart rate (‘Hr_std’); the other features depending on
357 frequency domain analysis require longer temporal analysis windows and could not be calculated
358 (60s at least - Shaffer & Ginsberg, 2017). RSP features were calculated using the BioSPPy library,
359 based on a detection algorithm for respiratory cycles, amplitudes, and phases (inspirations and
360 expirations). Following the pre-test phase, it was observed that the frequency of the car movements
361 at 0.2Hz imposed a specific respiration rate, which is precisely why additional features not
362 impacted by the car movements were calculated and investigated. With respiratory amplitude, the
363 magnitude of each breathing phase was calculated by measuring the difference between the peak
364 and trough of each breath in the respiration signal. Maximum inspiration (‘In_max’) and expiration
365 (‘Out_max’) were chosen for analysis. The overall EDA signal was obtained from the fluctuation
366 of two underlying components: one is a slower and steady baseline tonic component (skin
367 conductance level (SCL)) and the other is a faster or reactive phasic component (skin conductance
368 response (SCR)). Using the NeuroKit library, two SCR features were extracted through the phasic
369 component: peak indexes and SCR amplitudes. SCR amplitude was a change relative to the
370 deflection in the signal from onset to peak response. Mean SCR amplitude (‘SCR_mean’) and
371 standard deviation (‘SCR_std’) were chosen for analysis. For each channel and feature, the mean
372 and standard deviations were extracted over the different recording periods of interest to examine
373 changes over time in the sample.

374 6. Statistical analysis

375 Several dependent variables were analyzed at full sample level: (i) car sickness ratings (CSR),
376 (ii) features of the ECG recordings (‘Hr_mean’ and ‘Hr_std’), (iii) features of the RSP recordings
377 (‘In_max’ and ‘Out_max’), and (iv) features of the SCR recordings (‘SCR_mean’ and ‘SCR_std’).
378 The evolution of each dependent variable was compared against three independent variables:
379 ‘acceleration level’, ‘path predictability’, and ‘period’. For the ‘period’ variable, 6 periods were

380 defined: baseline period (Base), slalom period (S_{start} , S_{mid} , S_{stop} + S_{max}), and recovery period
381 (Recov).

382 First, car sickness ratings and the time to reach maximum CSR were analyzed during the S_{max}
383 period using a 2-level ('acceleration level': high and low) \times 2-level ('path predictability': regular
384 and unpredictable) repeated measures ANOVA. Secondly, the dynamics of changes in car sickness
385 ratings and physiological features were analyzed using a 2-level ('acceleration level': high and
386 low) \times 2-level ('path predictability': regular and unpredictable) \times 5-level ('period': Base, S_{start} , S_{mid} ,
387 S_{stop} and Recov) repeated measures ANOVA.

388 As a prior for all collected data, the condition of sphericity was also tested (Mauchly's test).
389 The p-value levels were corrected for possible deviations from sphericity by means of the Huynh–
390 Feldt epsilon (ϵ) (Kim et al., 2005; Ohyama et al., 2007; Benedek & Kaernbach, 2010; Dennison
391 et al., 2016). When significant differences were observed ($p < 0.05$), post-hoc analysis was
392 performed using a Fisher–Snedecor least significant difference test, allowing the results to be
393 refined by comparing the modalities two by two. For each significant effect, the effect size was
394 estimated using the partial eta squared (η^2).

395 Following these analyses, two-tailed Pearson correlation coefficients were calculated between
396 physiological measurements and maximum CSR for all conditions. Physiological measurements
397 were drawn from the S_{max} period and normalized from the Base period. Finally, stepwise multiple
398 linear regression analysis was performed to determine which physiological changes contributed to
399 the maximum CSR assessment. Only variables whose correlations with maximum CSR were
400 greater than 0.2 were selected for regression analysis.

401 All statistical analyses were performed using Statistica software® v.10 (Statsoft Inc, France).
402 Data are presented as mean \pm SEM for each assessment and significance levels as * $p < 0.05$, ** p
403 < 0.01 and *** $p < 0.001$.

404 **3 Results**

405 **3.1 CAN recordings**

406 All participants were subjected to a maximum of 26 slaloms during the slalom period. The
407 mean time for one slalom, the mean time for the whole slalom period, and the mean of the resulting
408 lateral oscillation frequencies and accelerations were calculated for each condition (Table 1).

Conditions	Mean time for 1 slalom (sec)	Mean time for slalom period (min)	Mean number of slaloms	Minimum number of slaloms	Lateral oscillation frequencies (Hz)	Lateral oscillation accelerations (m.s ²)
Regular Low (RL)	32 \pm 1	20 \pm 1	26 \pm 0.3	26	0.20 \pm 0.04	2.0 \pm 0.1

Unpredictable Low (UL)	32 ± 1	19 ± 3	25 ± 1.2	14	0.20 ± 0.04	3.0 ± 0.45
Regular High (RH)	35 ± 1	10 ± 7	13 ± 2.5	3	0.19 ± 0.04	5.5 ± 0.19
Unpredictable High (UH)	34 ± 1	11 ± 7	13 ± 2.9	2	0.19 ± 0.04	5.2 ± 0.28

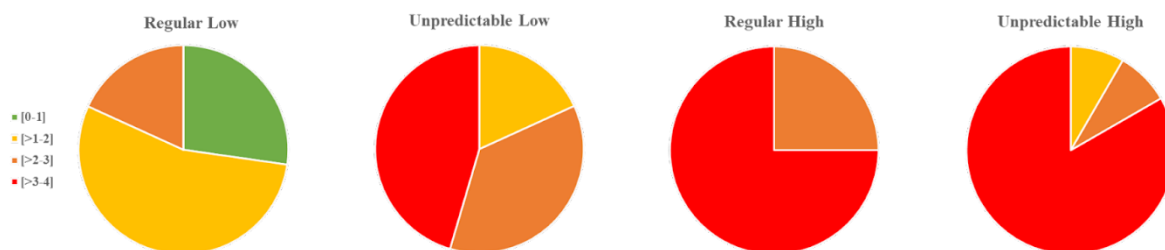
409

410 **Table 1:** Main characteristics of Regular Low (RL), Unpredictable Low (UL), Regular High (RH), and Unpredictable
 411 High (UH) slaloms experienced by the participants (mean ± SD). Note that the same ranges of mean lateral oscillation
 412 frequency and accelerations were applied in Regular and Unpredictable conditions.

413 3.2 Car sickness ratings (CSR)

414 3.2.1 Maximum CSR

415 During the test, all participants reported at least some degree of car sickness and reached their
 416 maximum CSR during the S_{max} period. The maximum ratings distribution for each condition is
 417 shown in Figure 3. High conditions led to a distribution with more high scores [3-4] than Low
 418 conditions (RH: +75% vs RL and UH: +39% vs UL). Unpredictable conditions had a distribution
 419 with more high scores than Regular conditions for both acceleration levels (UH: +8% vs RH and
 420 UL: +45% vs RL) (Fig 4). For an approximately similar level of acceleration ($\approx 5 \text{ m.s}^2$), there were
 421 more high scores in the UH condition than in the RH condition.



422

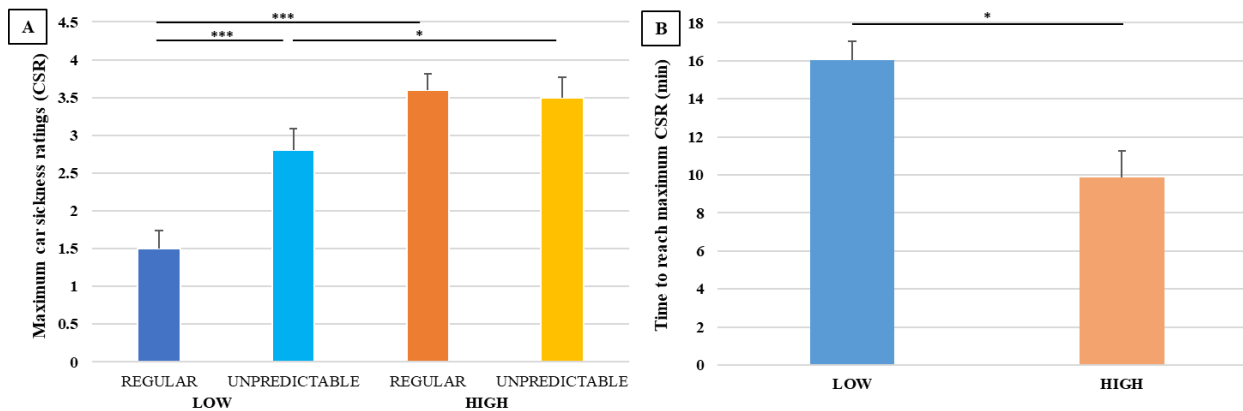
423

424 **Figure 4:** Distribution of maximum CSR reached by participants during the S_{max} period: green [0-1], yellow [1-2],
 425 orange [2-3], and red [3-4] (n=23).

426 Statistical analysis indicated a significant interaction effect between 'acceleration level' and 'path
 427 predictability' on maximum CSR measured in the S_{max} period ($F_{(1,21)} = 9.03$; $\epsilon = 1.0$; $p < 0.01$; $\eta^2 =$
 428 0.30). Post-hoc analyses revealed higher ratings in High conditions than in Low conditions ($p <$
 429 0.001) and higher ratings in UL than in RL ($p < 0.05$) (Fig 5 A). In addition, a significant effect of
 430 'acceleration level' was observed on the time taken to reach maximum CSR ($F_{(1,21)} = 7.09$; $\epsilon = 1.0$; p
 431 < 0.05 ; $\eta^2 = 0.25$). Participants reached their maximum score faster in High conditions than in
 432 Low conditions (Fig 5 B). All results (mean ± SEM) obtained for each feature by test period (S_{max} ,

433 Base, S_{start} , S_{mid} , S_{stop} , and Recov) can be found in supplementary material (Table 1). Details of all
 434 associated statistics are reported in Table 2 and supplementary material.

435
 436 **Figure 5:** (A) Maximum CSR observed for each condition in S_{max} period (B); time to reach maximum CSR (mean \pm



437 SEM; n=23). Statistical differences between conditions are shown by black stars and full lines. * significant difference
 438 ($p < 0.05$), *** significant difference ($p < 0.001$).

439

Three-factor ANOVA

	ACCEL	PATH	PERIOD	PATH*ACCEL	PERIOD*ACCEL	PATH*PERIOD	PATH*PERIOD*ACCEL
CSR	F(1,21) 20.19***	F(1,21) 9.08**	F(3,63) 60.45***	F(1,21) 4.76*	F(3,63) 10.60***	F(3,63) 2.90*	F(3,63) 5.61**
HR_mean	F(1,21) 0.00	F(1,21) 0.17	F(4,84) 20.02***	F(1,21) 0.28	F(4,84) 5.60***	F(4,84) 3.41*	F(4,84) 1.04
HR_std	1.65	0.61	2.44	0.60	3.21*	1.04	0.72
In_max	9.44**	2.50	17.34***	9.22**	3.60**	1.47	1.71
Out_max	9.00**	2.60	20.65***	9.55**	5.42***	3.13*	3.64**
SCR_mean	0.06	1.91	4.87**	0.43	1.92	1.05	0.47
SCR_std	0.65	3.93	6.51***	0.51	0.27	0.26	1.03

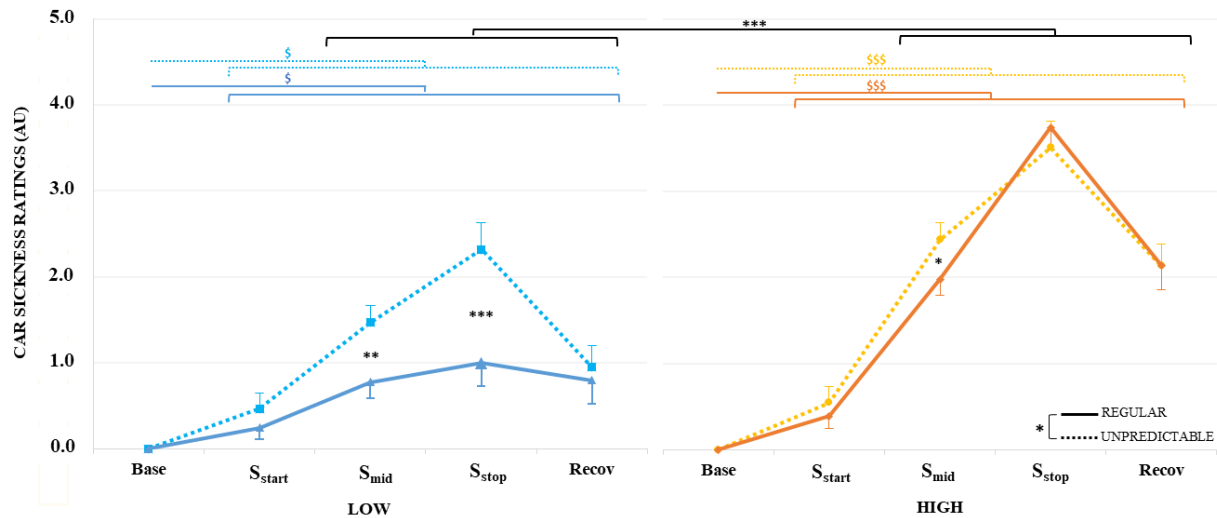
440

441 **Table 2:** Results of ANOVA analysis for each feature and each test period (Base, S_{start} , S_{mid} , S_{stop} and Recov) in each
 442 condition (mean \pm SEM; n=23). The three independent variables are: ACCEL=acceleration level, PATH=path
 443 predictability, and PERIOD=test period.

444 3.2.2 CSR dynamics

445 A significant interaction between 'test period', 'acceleration level', and 'path predictability' was
 446 observed on car-sickness rating dynamics ($F(3,63) = 5.61$; $\epsilon = 0.91$; $p < 0.01$; $\eta^2 = 0.49$). Post-
 447 hoc analyses revealed that 'Base' and ' S_{start} ' were not significantly affected. As illustrated in Figure
 448 6, each participant began the experiment symptom-free ('Base') and ratings did not significantly
 449 differ between conditions at ' S_{start} '. However, during the slalom period, ratings increased more or
 450 less sharply depending on conditions. There were significant differences between Low and High
 451 conditions ($p < 0.001$), with significantly higher ratings at ' S_{mid} ', ' S_{stop} ', and 'Recov' in the High

452 conditions than in the Low conditions. In addition, there were significant differences between
 453 Regular and Unpredictable conditions ($p < 0.05$) (Table 2 – 3). Ratings were significantly higher
 454 at 'S_{mid}' and 'S_{stop}' in the UL conditions than in the RL conditions, and were also higher at 'S_{mid}' in
 455 the UH conditions than in the RH conditions (Table 2 – 3). Whatever the condition, none of the
 456 ratings returned to baseline level at 'Recov'.

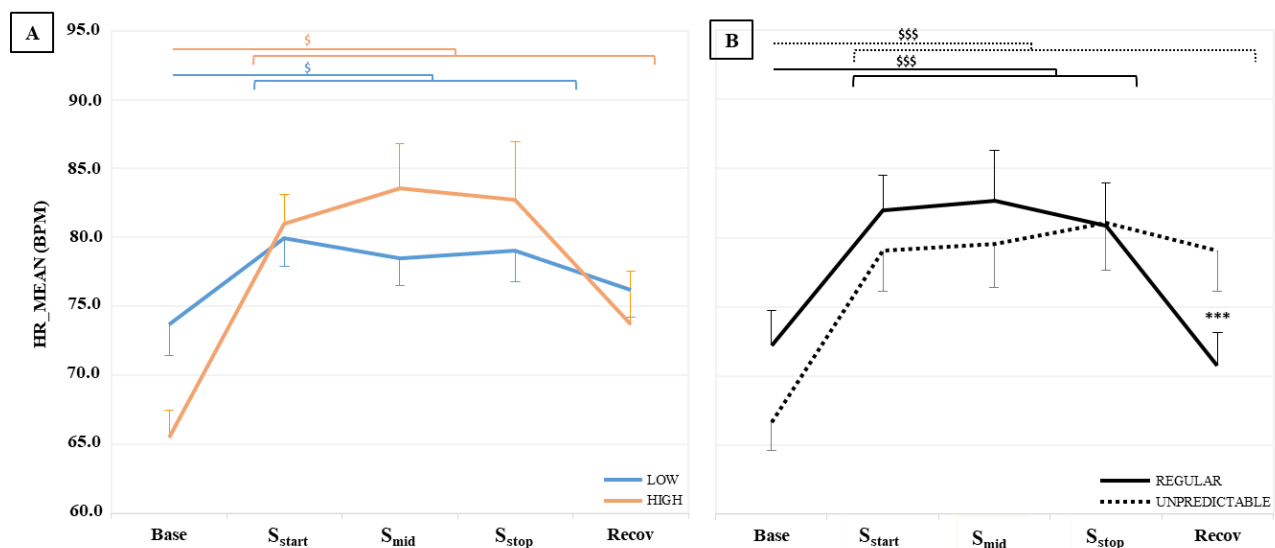


457
 458 **Figure 6:** CSR observed for each test period (Base, S_{start}, S_{mid}, S_{stop}, and Recov) in each condition (mean ± SEM;
 459 n=23). Statistical differences between test periods in a condition are shown by dollar symbols and lines color-coded
 460 by condition: (i) Regular Low: dark blue solid line, (ii) Unpredictable Low: light blue dashed line, (iii) Regular High:
 461 dark orange solid line, and (iv) Unpredictable High: light orange dashed line. Statistical differences between conditions
 462 are shown by black stars and full lines. * and \$ significant difference ($p < 0.05$), ** significant difference ($p < 0.01$),
 463 *** and \$\$\$ significant difference ($p < 0.001$).

464 **3.3 Physiological measurements**

465 3.3.1 ‘Hr_mean’ dynamics

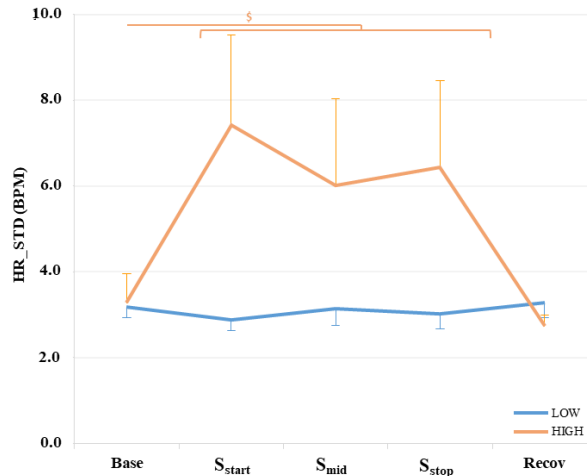
466 A significant interaction between 'test period' and 'acceleration level' was observed on mean
 467 heart rate ('Hr_mean') values ($F(4,84) = 5.56; \epsilon = 0.46; p < 0.01; \eta^2 = 0.21$). Post-hoc analyses
 468 revealed a significant increase in all values during the slalom period compared to baseline (Figure
 469 7A). During the recovery period, only Low condition values returned to baseline level (Table 2-
 470 3). Another significant interaction was observed between 'test period' and 'path predictability' on
 471 mean heart rate ('Hr_mean') values ($F(3,63) = 5.61; \epsilon = 0.36; p < 0.05; \eta^2 = 0.14$). Post-hoc
 472 analyses revealed a significant increase in all values during the slalom period compared to baseline
 473 (Figure 7B). In addition, there was a significant difference between Regular and Unpredictable
 474 conditions for the recovery period ($p < 0.01$) (Table 2 – 3), with higher values in Unpredictable
 475 conditions than in Regular conditions.



476 **Figure 7:** Representation of ‘Hr_mean’ values (mean ± SEM ; n=23) for (A) interaction between 'test period' and
 477 'acceleration level' and (B) interaction between 'test period' and 'path predictability' in each test period (Base, S_start,
 478 S_mid, S_stop, and Recov). Statistical differences between test periods in a condition are shown by dollar symbols and
 479 lines color-coded by condition: (i) Regular: black full line, (ii) Unpredictable: black dashed line, (iii) Low: light blue
 480 full line, and (iv) High: light orange full line. Statistical differences between conditions are shown by black stars. *
 481 and \$ significant difference ($p < 0.05$), *** and \$\$\$ significant difference ($p < 0.001$).

482 3.3.2 ‘Hr_std’ dynamics

483 A significant interaction between 'test period' and 'acceleration level' was observed for standard
 484 deviation of the heart rate ('Hr_std') values ($F(4,84) = 3.21; \epsilon = 0.40; p < 0.05; \eta^2 = 0.07$). For
 485 the High conditions, post-hoc analyses revealed a significant increase during the slalom period
 486 compared to baseline ($p < 0.01$) (Figure 8). During Recov, values returned to baseline level
 487 (Supplementary Table 1).

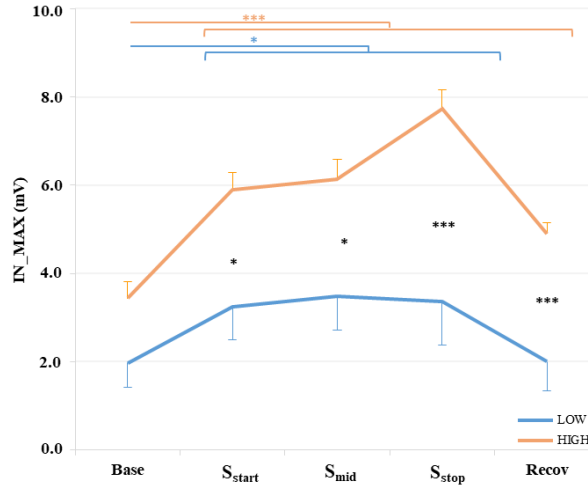


488

489 **Figure 8:** 'Hr_std' values observed for each test period (Base, S_start, S_mid, S_stop and Recov) according to 'acceleration
 490 level', regardless of 'path predictability' (mean \pm SEM; High conditions n =12; Low conditions n =11). Statistical
 491 differences between test periods in High conditions are indicated by a light orange dollar symbol and full lines. \$
 492 significant difference ($p < 0.05$)

493 3.3.3 'In_max' dynamics

494 A significant interaction between 'acceleration level' and 'path predictability' was observed for
 495 maximum inspiration ('In_max') values ($F(1,21) = 9.22$; $\epsilon = 0.96$; $p < 0.01$; $\eta^2 = 0.30$). Post-hoc
 496 analyses revealed higher values in the RH conditions than in the others (Figure 9). There was
 497 another significant effect of interaction between 'test period' and 'acceleration level' on maximum
 498 inspiration ('In_max') values ($F(4,84) = 3.60$; $\epsilon = 0.82$; $p < 0.01$; $\eta^2 = 0.15$). For both acceleration
 499 levels (Low and High), post-hoc analyses revealed a significant increase in all values during the
 500 slalom period compared to baseline (Figure 9). The increase was significantly higher in High
 501 conditions than in Low conditions for all slalom periods; values were also higher during the
 502 recovery period in High than in Low conditions. In High conditions, the values peaked at 'S_stop'
 503 and decreased during Recov but remained higher than baseline values. In Low conditions, no
 504 difference between slalom periods (S_start, S_mid, S_stop) was observed but values returned to baseline
 505 level during Recov.

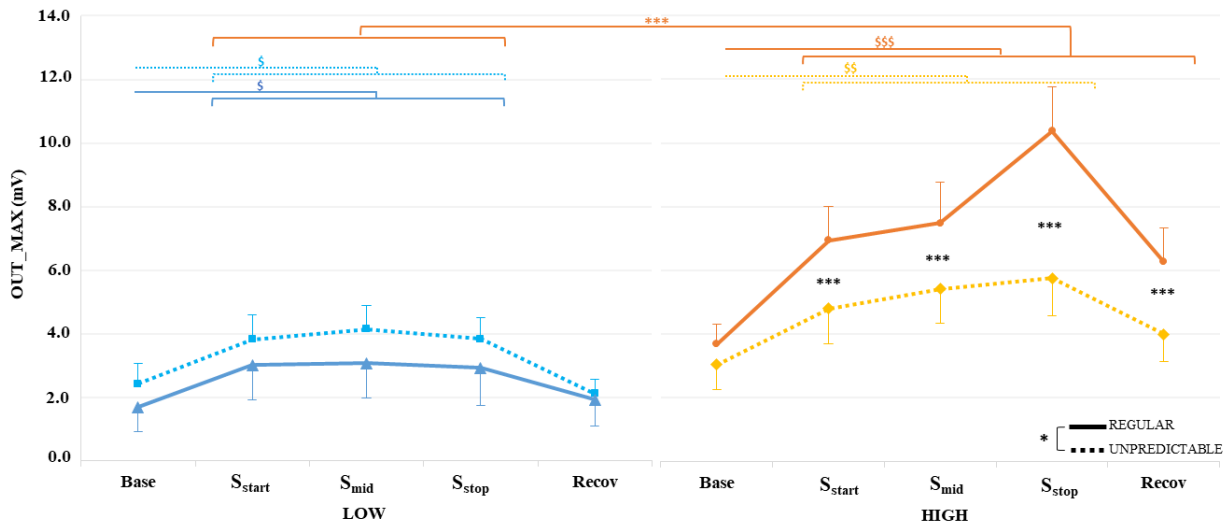


507 **Figure 9** : 'In_max' values observed for each test period (Base, S_start, S_mid, S_stop, and Recov) according to acceleration
 508 level, regardless of path predictability (mean \pm SEM; High conditions n =12; Low conditions n =11). Statistical
 509 differences between test periods in a condition are shown by dollar symbols and lines color-coded by condition: (i)
 510 Low : light blue full line and (ii) High : light orange full line. Statistical differences between conditions are shown by
 511 black stars. * and \$ significant difference ($p < 0.05$), *** and \$\$\$ significant difference ($p < 0.001$).

512 3.3.4 'Out_max' dynamics

513 A significant effect of interaction between 'test period', 'acceleration level', and 'path
 514 predictability' was observed on maximum expiration ('Out_max') values ($F(4,84) = 3.64$; $\epsilon = 1.0$;
 515 $p < 0.01$; $\eta p^2 = 0.30$). Post-hoc analyses revealed that 'Base' values were not significantly affected
 516 by the factors (Figure 10). In contrast, during the slalom period, all values increased similarly
 517 compared to baseline, except in RH conditions, where significantly higher values were observed
 518 during slaloms and Recov than in the other conditions (Table 2 – 3). During Recov, only RH
 519 condition values did not return to baseline level.

520



521

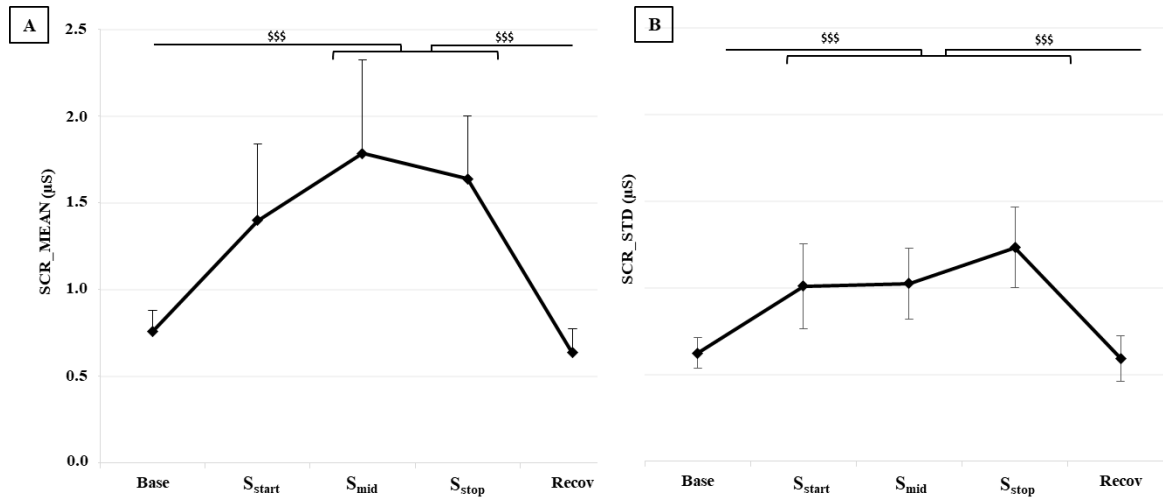
522 **Figure 10:** ‘Out_max’ values observed for each test period (Base, S_start, S_mid, S_stop, and Recov) in each condition (mean
 523 ± SEM; n=23). Statistical differences between test periods in a condition are shown by dollar symbols and lines color-
 524 coded by condition: (i) Regular Low : dark blue full line, (ii) Unpredictable Low : light blue dashed line, (iii) Regular
 525 High : dark orange full line, (iv) Unpredictable High : light orange dashed line. For the Regular High condition,
 526 statistical differences between test periods and from other conditions are shown by dark orange stars and full lines.
 527 Statistical differences between conditions are shown by black stars. * and \$ significant difference (p < 0.05), ** and
 528 \$\$ significant difference (p < 0.01), *** and \$\$\$ significant difference (p < 0.001).

529 3.3.5 ‘SCR_mean’ dynamics

530 A significant main effect of ‘test period’ was observed on mean values for skin conductance
 531 response (‘SCR_mean’) (F(4, 84) = 4.87; ε = 0.71; p < 0.01; ηp2 = 0.19). Post-hoc analyses revealed
 532 a significant increase during S_mid and S_stop compared to baseline (Figure 11 A). Finally, stopping
 533 the slalom during Recov induced a significant decrease in values, which returned to baseline level.

534 3.3.6 ‘SCR_std’ dynamics

535 A significant effect of ‘test period’ was observed on the standard deviation of skin conductance
 536 response (‘SCR_std’) (F(4, 84) = 6.51; ε = 0.91; p < 0.001; ηp2 = 0.24). Post-hoc analyses revealed
 537 significant increases throughout the slalom period compared to baseline (Figure 11 B). Stopping
 538 the slalom during Recov induced a significant decrease in values, which returned to baseline level.



539
 540
 541 **Figure 11:** (A) ‘SCR_mean’ and (B) ‘SCR_std’ values observed for each test period (Base, S_start, S_mid, S_stop, and Recov)
 542 regardless of path predictability (mean ± SEM; n =23). Statistical differences between test periods are shown in black.
 543 \$\$\$ significant difference (p < 0.001).

544 3.4 Relationship between car sickness ratings and physiological measurements

545 Significant correlations were observed between maximum CSR (CSR_max) and physiological
 546 parameters (Table 4 A). There were significant correlations between CSR_max and ‘HR_mean’
 547 and ‘Out_max’ values (greater than 0.4 for both), as well as with ‘HR_std’, and ‘In_max’ (greater
 548 than 0.2 for both). These results suggest that the changes observed in cardiac and respiratory
 549 measurements and car-sickness symptoms are linked. In order to confirm this hypothesis, a
 550 regression analysis was performed to determine which physiological changes could be used to
 551 estimate maximum CSR during S_max. ‘HR_mean’, ‘HR_std’, ‘In_max’, and ‘Out_max’ showed
 552 adequate predictive power for inclusion in the regression. It was found that increases in car-
 553 sickness symptoms can be estimated from changes in cardiac and breathing activities. Indeed,
 554 ‘HR_mean’, ‘HR_std’, and ‘Out_max’ explained 41.4% (adjusted R² = 0.372) of the variance in
 555 maximum CSR values, (F(3,42) = 9.899, σ_{est} = 0.898, p < 0.001) (Table 4 B).

A	HR_mean	HR_std	In_max	Out_max	SCR_mean	SCR_std
CSR_max	0.466*	0.294*	0.359*	0.442*	0.171	-0.081

B	β	t	Std. Error	p
HR_mean	0.454	3.762	0.012	0.001
HR_std	0.238	1.860	0.054	0.070
Out_max	0.299	2.331	0.045	0.025

556 **Table 4:** Results of (A) Pearson correlations between maximum CSR and physiological measurements and (B)
 557 Stepwise regression of physiological measurements on maximum CSR (Criterion to enter = 0.2). (n=23) * p < .05
 558 (two-tailed)

559 4 Discussion

560 For the first time in real driving conditions, our results show that sickness-inducing stimuli
561 such as increased lateral acceleration and vehicle path unpredictability induce (i) an increase in
562 symptom severity and (ii) specific physiological changes reflecting the activation of the SNS. CSR
563 results reveal that the greater the lateral acceleration and the less predictable the vehicle path, the
564 stronger the symptoms. Moreover, an increase in several physiological parameters is observed
565 simultaneously with the increase in CSR, with moderate positive correlations between CSR
566 evolution and physiological changes. Furthermore, linear regression results suggest that these
567 physiological parameters can be used to detect car sickness, thus demonstrating a link between car
568 sickness symptoms and physiological changes.

569 4.1 Triggers of car sickness

570 While the impact of acceleration in the vertical and longitudinal axes has been thoroughly
571 documented, few studies have investigated the lateral axis. Yet lateral acceleration has been
572 identified as the most nauseating in cars (Cheung & Nakashima, 2006; Diels, 2014; Smyth et al.,
573 2021). Indeed, our finding that the higher the level of lateral acceleration, the stronger the car
574 sickness symptoms extends those of previous work (Turner, 1999; Feng, 2017; Irmak, 2021), this
575 time in the lateral axis and in real driving conditions. During the slalom period, participants
576 exhibited a greater distribution of high CSR in High conditions than in Low conditions (RH: +75%
577 vs RL and UH: +39% vs UL). In addition, participants recorded higher maximum CSR and reached
578 this maximum earlier in High conditions (both Regular and Unpredictable) than in Low conditions.
579 These results are consistent with previous findings on longitudinal acceleration. By increasing
580 acceleration level in a dynamic simulator, Irmak et al. (2022) showed that maximum ratings not
581 only increased but also were reached earlier, since their dropout rates increased. Regarding CSR
582 dynamics, a significant increase was observed with time from S_{mid} onwards, reaching a maximum
583 at ' S_{stop} '. Furthermore, the symptoms that developed during the slalom period, although attenuated,
584 persisted into the recovery period ($CSR \neq 0$). These results extend results of previous papers
585 showing that car sickness severity increases throughout testing (Kuiper et al., 2018; Irmak, 2021;
586 Henry et al., 2022) and that symptoms can persist from minutes to hours after stimulation (Kim et
587 al., 2005; Golding, 2006; Diels & Bos, 2016). However, we showed more specifically that high
588 acceleration levels lead to a sharper increase in symptom severity, which remains higher during
589 the post-stimulation recovery period. Our results demonstrate that there is a strong relationship
590 between levels of lateral acceleration in cars and increased car sickness (timing and severity).

591 Determining what kind of lateral movements to avoid in future autonomous vehicles means
592 exploring their separate impacts and parameters (acceleration, direction, frequency etc.). Our study
593 employed the frequency known to induce maximum nausea in cars (Wada et al., 2012; Wada &
594 Yoshida, 2016; Henry et al., 2022) regardless of acceleration level. Here, we show that increasing
595 the level of acceleration in cars with sinusoidal lateral movements at this 0.2 Hz frequency leads

596 to more severe symptoms. This extends results obtained with the Mc Cauley (1974) model applied
597 to sinusoidal vertical movements (O’Hanlon & McCauley, 1974; Bos & Bles, 1998). At 0.2 Hz,
598 Bos and Bles (1998) obtained more than 80 % MSI at 5m/s², as opposed to around 60 % at 2 m/s².
599 Our similar observations appear to suggest that acceleration level has a similar impact in the three
600 axes (lateral, longitudinal, and vertical) at 0.2 Hz. Likely, the otolith tilt/translation ambiguity
601 (Wood, 2002; Clément, 2011) induced at this 0.2 Hz frequency is amplified by the increase in
602 acceleration level, whatever the direction of application. The vestibular system is known to be
603 particularly sensitive to changes in velocity, i.e., accelerations (Mayne, 1974; Reason & Brand,
604 1975; Kuiper, Bos, Schmidt, et al., 2020b). When the acceleration level increases, the vestibular
605 system thus becomes highly engaged and may be largely responsible for the worsening of the
606 sensory conflict causing car sickness.

607 Our study also investigated, for the first time in real driving conditions, the impact of car
608 path unpredictability on symptom severity. Interestingly, our results show that inability to predict
609 vehicle path also exacerbates symptoms. Unpredictable conditions had a CSR distribution with
610 more high scores than Regular conditions. More precisely, high scores appeared more frequently
611 in UH conditions than in RH conditions at almost the same levels of acceleration ($\approx 5\text{m.s}^2$). In
612 addition, maximum CSR were greater in Unpredictable than in Regular at low acceleration levels.
613 Furthermore, CSR were higher in ‘S_{mid}’ and ‘S_{stop}’ for UL conditions than for RL conditions and
614 higher in ‘S_{mid}’ for UH conditions than for RH. Thus, inability to predict vehicle trajectories
615 induced a gradual increase in symptom severity during the stimulation period. These results from
616 real car lateral accelerations are in line with those obtained in the laboratory along the longitudinal
617 axis using repeated fore-aft motion on a sled (Kuiper, Bos, Schmidt, et al., 2020b). Movements in
618 response to events unpredictable either in timing or direction caused more severe motion sickness
619 symptoms than when the same events occurred in a predictable way. In contrast, other studies on
620 movement predictability have focused on the effectiveness of countermeasures allowing
621 participants to anticipate future movements based on auditory (Kuiper, Bos, Diels, et al., 2020a;
622 Maculewicz et al., 2021), visual (Hendricks & Tumpey, 1990) or multimodal cues (Sweeney &
623 Bartell, 2017). Overall, they report less severe motion sickness symptoms when participants are
624 able to anticipate future movements with help. However, these studies manipulated the
625 participants’ ability to anticipate events, whereas our study manipulated the events themselves so
626 as to make them unpredictable for the participants.

627 Nevertheless, both mechanisms depend on the updating of internal models according to the
628 theory of sensory mismatch (Bos & Bles, 2002; Bos et al., 2008, 2010; Dennison et al., 2016).
629 This theoretical framework explains why drivers do not experience motion sickness, whereas
630 passengers do (Bos et al., 2008). Drivers can predict vehicle path (acceleration, speed, direction),
631 which allows them to update their internal models and predict self-motion using efference copies
632 (Reason & Brand, 1975; Bles et al., 1998; Bos & Bles, 1998; Bos et al., 2008). Typically, when
633 the forward internal model is correctly tuned, the expected movements coincide with the perceived
634 movements. Passengers however, in the absence of external help (anticipatory cues), are unable to

635 predict upcoming movements. In addition, when passengers expect regular movements and the
636 driver performs unpredictable movements, the mismatch between expected and real movements is
637 amplified, and the internal model cannot be properly tuned. This may explain why our study found
638 that participants became sicker in unpredictable conditions, consistent with the idea that a major
639 cause of motion sickness is a mismatch between perceived and expected motion (Reason & Brand,
640 1975; Bles et al., 1998; Kuiper, Bos, Schmidt, et al., 2020b).

641 **4.2 Physiological Measures**

642 As previously mentioned, the literature on physiological measurements and motion
643 sickness indicates that (i) there is as yet no consensus on an objective indicator of motion sickness,
644 (ii) despite the number of studies, there is no consensus on the directions (decrease/increase) of
645 the physiological changes themselves, and (iii) so far, most studies have been conducted in
646 laboratory conditions (rotating optokinetic drum, VR, Static driving simulator, etc.). Therefore,
647 the third objective of this study was to investigate the relationship between car sickness and
648 physiological responses in real driving conditions. We first analyzed the dynamics of physiological
649 parameters retained over the several test phases to compare their evolution with CSR dynamics.
650 Overall, the physiological parameters uniformly showed an significant evolution during the slalom
651 period, whereas responses during the recovery period were not homogeneous.

652 'HR_mean' and 'HR_std' reflect modulations of cardiac activity and its variability during
653 the test (Shaffer & Ginsberg, 2017; Meteier et al., 2021). 'HR_mean' showed a significant increase
654 during the slalom period in all conditions and a return to baseline level only in Low and Regular
655 conditions during the recovery period. This suggests that the most sickness-inducing conditions
656 had the most persistent effects on cardiac activity. 'HR_std' showed an increase in High conditions
657 during the slalom period, with a subsequent return to baseline level, indicating that changes were
658 only induced by high levels of acceleration and did not persist over time. These increases could be
659 interpreted as only due to the vehicle's movements and not to the evolution of the sickness.
660 However, cardiac activity was elevated during the full slalom period, simultaneously with
661 increased car sickness; for the most sickness-inducing stimuli, this persisted in the recovery period.
662 Type of stimulation therefore has an impact on 'HR_mean' that may persist once the movements
663 stop, indicating that the changes are not solely caused by the agitation experienced. Indeed, we
664 observed a significant correlation between 'HR_mean', 'HR_std' values and the most severe car
665 sickness (CSR_max): increases in car sickness severity were accompanied by increased cardiac
666 activity. Our findings confirm the hypothesis of a relationship between car sickness and cardiac
667 changes (Keshavarz et al., 2022), although findings in the literature remain inconsistent. This
668 discrepancy is mainly due to the kind of stimuli employed, and/or the methodology used for
669 measuring and analyzing cardiac activity. Several studies on cardiac parameters used laboratory
670 setups, with inconclusive results (increase, decrease, no change) (Hu et al., 1991; Cheung, 2004;
671 Kim et al., 2005; Dahlman et al., 2009; Koohestani et al., 2019). Only one study measured
672 physiological variables in cars, reporting a slight increase in heart rate with car movements (Irmak,

673 2021). Yet the stimuli used were similar to those in our study, with a lateral acceleration of almost
674 4m/s^2 (i.e., between our low and high conditions), and a condition with no view of the outside
675 environment was used (i.e., highly sickness-inducing). Comparing our results with the literature
676 reveals that the direction and magnitude of cardiac changes likely depends on the experimental
677 environment and especially on the nature of the stimulus itself (frequency, acceleration, speed,
678 direction).

679 Regarding RSP parameters, we analyzed maximum inspiration ('In_max') and expiration
680 ('Out_max') values, reflecting respiratory volume. Although these features are not well
681 documented in the literature, they proved relevant in our study. As with cardiac parameters, an
682 increase in both was observed during the slalom period for all conditions. 'In_max' values revealed
683 a gradual and strong increase until 'S_{stop}' in High conditions only, while 'Out_max' values
684 exhibited the same pattern in RH conditions only. In the same vein, during the recovery period,
685 respiratory measurements remained high only in High conditions for 'In_max' and in RH
686 conditions for 'Out_max'. This provides evidence that higher lateral acceleration levels induce
687 greater and more persistent changes in breathing volume. The positive correlation observed
688 between our breathing parameters and the most severe car sickness (CSR_max) confirms this
689 observation. This relationship is also supported by studies demonstrating that controlled breathing
690 can reduce the level of motion sickness (Yen Pik Sang et al., 2003; Denise et al., 2009; Chin-Teng
691 Lin et al., 2011). Lin et al., (2011) showed that people affected by motion sickness make breathing
692 adjustments (deep breathing) to relieve their discomfort. However, in our study, while some
693 increase in breathing volume was observed, these adjustments remained limited, mainly due to the
694 car movements. In fact, we found that the frequency of car movements at 0.2Hz imposed a specific
695 respiration rate, which could partly explain why symptoms remained so severe: participants were
696 not in full control of their breathing. Furthermore, in the regular conditions, participants could take
697 advantage of periods with less stimulation (between turns) to adapt their breathing through greater
698 inspiration and expiration. In contrast, our results tend to indicate that there were even fewer
699 adjustments under unpredictable car movements, especially with high acceleration levels. All these
700 observations argue for the hypothesis that physiological changes under sickness-inducing
701 conditions depend on the nature of the stimulus.

702 Finally, we analyzed the EDA parameters 'SCR_mean' and 'SCR_std', the mean and
703 variability of phasic skin conductance responses. This electrodermal conductance is used to
704 measure sweating, a major motion sickness symptom (Kennedy et al., 2010; Lackner, 2014). Our
705 SCR values increased during the slalom period and returned to baseline level during the recovery
706 period. Under stimulation, 'SCR_mean' showed an increase from 'S_{mid}' to 'S_{stop}' and 'SCR_std'
707 showed an increase from 'S_{start}' to 'S_{stop}'. These results are in agreement with those of Irmak et al.
708 (2021), also obtained in a real car: sickness-inducing movements increased electrodermal
709 conductance in palmar sites over time. The literature generally reports the same observation with
710 increased severity of motion sickness (Hu et al., 1991; Harm, 2002; Kim et al., 2005). While it has
711 been shown that forehead measurements gave highly sensitive measurements (Golding, 1992; Wan

712 & Hu, 2003), our results confirmed that measurements on palmar fingers also led to high satisfying
713 sensibility. However, explanations for the underlying mechanisms remain unclear and
714 inconsistent, possibly due to the varying measurement sites (forehead, finger, back of hand) and
715 features used.

716 We observed several physiological changes when participants were affected by car
717 sickness. There is a consensus among certain studies that all kinds of motion sickness can be
718 considered as a stress response to a stressful stimulus (sickness-inducing movements) inducing
719 particular physiological changes (Harm, 2002; Napoletano & Rossi, 2018). An increase in
720 cardiovascular, respiratory, and/or electrodermal activities, as in our study, has previously been
721 shown to reflect physiological stress (Cacioppo et al., 2007). It is known that depending on the
722 stress or agitation level of the person, the homeostasis of the body is modulated, causing an
723 alternation between the activation of the sympathetic and parasympathetic systems (Shaffer &
724 Ginsberg, 2017). However, under severe stimulus, the sympathetic nervous system (SNS) dictates
725 appropriate mechanisms and physiological responses to enhance the body's ability to deal with a
726 threat (known as the "fight or flight response") (Harm, 2002; Irmak, 2021). Notably, this is
727 achieved through increased arousal, which modifies electrodermal conductance (EDA), strongly
728 correlated with the activity of the sweat glands (sweating) (Boucsein, 2012). It also increases the
729 heart and respiratory rate, which amplifies the blood flow and enhances the transport and supply
730 of oxygen in the body (Cacioppo et al., 2007; Chan et al., 2022). Therefore, our results seem to
731 highlight a specific/dominant activation of the sympathetic system during the progression of car
732 sickness symptoms. Nevertheless, motion sickness is more complex than a simple stress and/or
733 agitation episode, which is why other studies contest the ability of physiological measurements
734 alone to indicate motion sickness levels (Keshavarz et al., 2022; Smyth et al., 2021). Actually, the
735 literature has illustrated the difficulty and unreliability of relating physiological measurements to
736 motion sickness, depending on the environment and stimuli used (Dennison et al., 2016;
737 Koohestani et al., 2019; Keshavarz et al., 2022). In our study, although the magnitude of our
738 cardiac and respiratory changes depended on the stimuli used (4 conditions), all parameters
739 evolved in the same direction and correlatively with car sickness severity. Moreover, the linear
740 regression showed that our measures (cardiac and respiratory) could explain 41% of the variance
741 in maximum CSR values, demonstrating the link between the physiological state involved in car
742 sickness and its symptoms.

743 **4.3 Limitations of the study**

744 Our results should be interpreted with caution in view of certain limitations. One major
745 limitation of the study is sample size. Although the participants were selected for their high
746 susceptibility to motion sickness, our results showed inter-individual variability which limited our
747 data analyses (e.g., precise data temporal evolution, modeling, analysis per individual, etc.). More
748 data from a heterogeneous and larger population are needed before these findings can be
749 generalized. Second, this study is one of the first to measure physiological parameters in real

750 driving conditions, which is both a limitation and a challenge. Our environment, where noise could
751 impact the recorded data, the method of pre-processing and physiological feature extraction had
752 to be adapted in order to obtain clean and useful signals. In addition, new physiological features
753 not greatly affected by vehicle dynamics (respiration rate) were explored, reducing the scope for
754 comparison with previous laboratory studies. However, our findings point to the value of common
755 physiological measures, such as heart rate, already used in other motion sickness studies (Kim et
756 al., 2005; Dahlman et al., 2009; Dennison et al., 2016; Koohestani et al., 2019; Irmak, 2021), as
757 well as respiratory amplitude ('In_max' and 'Out_max'), as possible indicators of car sickness
758 occurrence. These encouraging results deserve to be further explored. Third, it should be noted
759 that when we manipulated vehicle path unpredictability, the acceleration level was also being
760 manipulated. Under high acceleration levels, almost all participants rapidly reached their
761 maximum symptoms (ratings of 4 = end of test). This saturation prematurely stopped the runs,
762 resulting both in a rating plateau (a floor effect (Levine et al., 2014; Irmak, 2021)) and in reduced
763 exposure time (≈ 10 min).-Thus, had a higher symptom threshold than 'mild to moderate nausea'
764 been applied, thereby lengthening exposure time, we might have observed a greater difference
765 between the regular and unpredictable conditions even at high acceleration levels. Finally, only
766 two lateral acceleration levels (2 m.s^2 and 5 m.s^2) and one frequency level (0.2Hz) were analyzed
767 in this study. Although this frequency is recognized in the literature as the most nauseating (Bos
768 & Bles, 1998), and the lateral acceleration levels assessed here induced symptoms, this was not
769 sufficient to allow proper analysis of the impact of vehicle dynamics in the different axes (lateral,
770 longitudinal and vertical). Adapting the model proposed by Bos and Bles (1998) for vertical
771 stimulations to car movements and determining the specific characteristics of movement causing
772 car sickness will require testing a larger range of accelerations (0 to 6m/s^2) and frequencies (0 to
773 0.7 Hz). Once the impact of car movements is known, more realistic studies on the road should be
774 considered.

775 **5 Conclusion**

776 For the first time in real driving conditions, our results show that the stronger the lateral
777 acceleration (2 vs 5 m.s^2), the more severe the symptoms of car sickness, and that inability to
778 predict the vehicle's path exacerbates symptoms. In future autonomous vehicles, the vehicle
779 dynamics will need to be designed, as far as possible, to limit nauseating movements such as high
780 lateral acceleration and/or low frequency movements. In addition, countermeasure solutions
781 should be considered to allow vehicle occupants to anticipate the vehicle's path in real time so as
782 to update their internal model. Furthermore, these particular factors, which are highly prevalent
783 during car travel, induce specific physiological changes reflecting SNS activation. It seems that
784 the more impactful the stimulus is considered by participants (high CSR), the more their SNS is
785 activated to allow the body to respond. Our work thus provides evidence that (i) physiological
786 changes related to motion sickness can be recorded in the car with laboratory devices, (ii)
787 processing stages need to be adapted according to these environmental constraints, (iii) some
788 features explored in the laboratory can also be used in a real car, but (iv) new features (In_max

789 and Out_max) also deserve to be explored and could reveal SNS activation. Indeed, the linear
790 regression applied to our data suggests that these physiological parameters can be used to confirm
791 the CSR level indicated by the participants. While the results of this study are encouraging,
792 however, using physiological measures alone to indicate car sickness symptoms does not currently
793 appear sufficient. Subjective measures such as ratings (CSR) still need to be used to evaluate car
794 sickness severity and to identify the physiological changes associated with it. Automating the
795 detection of car sickness from objective data only will require a predictive model taking into
796 account the individuals' parameters as well as the nature of the stimuli. For this purpose, further
797 research should be conducted to assess (i) the influence of other car-sickness-inducing factors
798 (different vehicle dynamics, levels of control and predictability, passenger positioning, etc.) and
799 (ii) the changes in individual parameters that these factors induce.

800 **Acknowledgments**

801 We thank Julien Bonnet (Stellantis) and Aurore Bourrelly for their help in the preparation
802 of this experiment. We are grateful to Telecom Paris Tech team as well as Rafik Belkacem and
803 Nadjet Hosni for their technical assistance with data analysis. Finally, we thank Marjorie Sweetko
804 for English language editing of the manuscript.

805 **Funding**

806 This study was conducted under a CIFRE thesis (N° 2018/1450 doctoral grant from
807 National Association for Research and Technology (ANRT)) and the OpenLab agreement
808 “Automotive Motion Lab” between Stellantis and Aix-Marseille University and CNRS.

809 **Ethics Statement**

810 This study was reviewed and approved by the Local Ethics Committee of Aix-Marseille
811 University in accordance with the ethical standards laid down in the 1964 Declaration of Helsinki.
812 The participants provided their written informed consent to participation in this study.

813 **Author Contributions**

814 All authors: Conceptualization, Methodology. Eléonore Henry and Clément Bougard:
815 Investigation, Formal analysis and Visualization. Eléonore Henry : Data Curation, Writing-
816 Original draft preparation. Clément Bougard, Christophe Bourdin and Lionel Bringoux
817 Supervision, Writing- Reviewing and Editing.

818 **Conflict of Interest**

819 The authors declare that the research was conducted in the absence of any commercial or
820 financial relationships that could be construed as a potential conflict of interest.

821 **6 Bibliography**

- 822 Aykent, B., Merienne, F., Guillet, C., Paillot, D., & Kemeny, A. (2014). Motion sickness evaluation and
823 comparison for a static driving simulator and a dynamic driving simulator. *Proceedings of the Institution*
824 *of Mechanical Engineers, Part D: Journal of Automobile Engineering*, 228(7), 818-829.
825 <https://doi.org/10.1177/0954407013516101>
- 826 Benedek, M., & Kaernbach, C. (2010). Decomposition of skin conductance data by means of nonnegative
827 deconvolution. *Psychophysiology*, 47(4), 647-658. <https://doi.org/10.1111/j.1469-8986.2009.00972.x>
- 828 Bles, W., Bos, J. E., de Graaf, B., Groen, E., & Wertheim, A. H. (1998). Motion sickness : Only one
829 provocative conflict? *Brain Research Bulletin*, 47(5), 481-487. [https://doi.org/10.1016/S0361-](https://doi.org/10.1016/S0361-9230(98)00115-4)
830 [9230\(98\)00115-4](https://doi.org/10.1016/S0361-9230(98)00115-4)
- 831 Bos, J. E., & Bles, W. (1998). Modelling motion sickness and subjective vertical mismatch detailed for
832 vertical motions. *Brain Research Bulletin*, 47(5), 537-542. [https://doi.org/10.1016/S0361-9230\(98\)00088-](https://doi.org/10.1016/S0361-9230(98)00088-4)
833 [4](https://doi.org/10.1016/S0361-9230(98)00088-4)
- 834 Bos, J. E., & Bles, W. (2002). Theoretical considerations on canal–otolith interaction and an observer
835 model. *Biological Cybernetics*, 86(3), 191-207. <https://doi.org/10.1007/s00422-001-0289-7>
- 836 Bos, J. E., Bles, W., & Groen, E. L. (2008). *A theory on visually induced motion sickness*. 11.
- 837 Bos, J. E., de Vries, S. C., van Emmerik, M. L., & Groen, E. L. (2010). The effect of internal and external
838 fields of view on visually induced motion sickness. *Applied Ergonomics*, 41(4), 516-521.
839 <https://doi.org/10.1016/j.apergo.2009.11.007>
- 840 Bos, J., Mackinnon, S., & Patterson, A. (2006). Motion Sickness Symptoms in a Ship Motion Simulator :
841 Effects of Inside, Outside and No View. *Aviation, space, and environmental medicine*, 76, 1111-1118.
- 842 Bos, J. E., Van Leeuwen, R. B., & Buintjes, T. D. (2018). Motion sickness in motion: from carsickness to
843 cybersickness. *Nederlands tijdschrift voor geneeskunde*, 162, D1760-D1760.
- 844 Boucsein, W. (2012). Principles of Electrodermal Phenomena. In W. Boucsein (Éd.), *Electrodermal*
845 *Activity* (p. 1-86). Springer US. https://doi.org/10.1007/978-1-4614-1126-0_1
- 846 Cacioppo, J., Tassinary, L., & Berntson, G. (2007). *Handbook of psychophysiology*.
847 <https://doi.org/10.13140/2.1.2871.1369>
- 848 Carreiras, C., Alves, A. P., Lourenço, A., Canento, F., Silva, H., & Fred, A. (2015). Biosppy : Biosignal
849 processing in python. *Accessed on*, 3(28), 2018.
- 850 Chan, P. Y., Ryan, N. P., Chen, D., McNeil, J., & Hopper, I. (2022). Novel wearable and contactless heart
851 rate, respiratory rate, and oxygen saturation monitoring devices : A systematic review and meta-analysis.
852 *Anaesthesia*, 77(11), 1268-1280. <https://doi.org/10.1111/anae.15834>
- 853 Chen, Y.-C., Duann, J.-R., Chuang, S.-W., Lin, C.-L., Ko, L.-W., Jung, T.-P., & Lin, C.-T. (2010). Spatial
854 and temporal EEG dynamics of motion sickness. *NeuroImage*, 49(3), 2862-2870.
855 <https://doi.org/10.1016/j.neuroimage.2009.10.005>
- 856 Cheung, B. (2004). *Physiological and behavioral responses to an exposure of pitch illusion in the simulator*.
857 *Aviation, space, and environmental medicine*. (75)8. P.657.

858 [https://sh2hh6qx2e.search.serialssolutions.com/?sid=google&auinit=B&aulast=Cheung&atitle=Physiologic+and+behavioral+responses+to+an+exposure+of+pitch+illusion+in+the+simulator&title=Aviation,+s](https://sh2hh6qx2e.search.serialssolutions.com/?sid=google&auinit=B&aulast=Cheung&atitle=Physiologic+and+behavioral+responses+to+an+exposure+of+pitch+illusion+in+the+simulator&title=Aviation,+space,+and+environmental+medicine&volume=75&issue=8&date=2004&spage=657&issn=0095-6562)
859 [pace,+and+environmental+medicine&volume=75&issue=8&date=2004&spage=657&issn=0095-6562](https://sh2hh6qx2e.search.serialssolutions.com/?sid=google&auinit=B&aulast=Cheung&atitle=Physiologic+and+behavioral+responses+to+an+exposure+of+pitch+illusion+in+the+simulator&title=Aviation,+space,+and+environmental+medicine&volume=75&issue=8&date=2004&spage=657&issn=0095-6562)
860

861 Cheung, B., & Nakashima, A. (2006). *A Review on the Effects of Frequency of Oscillation on Motion*
862 *Sickness*. 29.

863 Chin-Teng Lin, Chun-Ling Lin, Tzai-Wen Chiu, Jeng-Ren Duann, & Tzyy-Ping Jung. (2011). Effect of
864 respiratory modulation on relationship between heart rate variability and motion sickness. *2011 Annual*
865 *International Conference of the IEEE Engineering in Medicine and Biology Society*, 1921-1924.
866 <https://doi.org/10.1109/IEMBS.2011.6090543>

867 Chourpiliadis, C., & Bhardwaj, A. (2023). Physiology, Respiratory Rate. In *StatPearls*. StatPearls
868 Publishing. <http://www.ncbi.nlm.nih.gov/books/NBK537306/>

869 Clément, G. (2011). *Fundamentals of Space Medicine*. Springer New York. [https://doi.org/10.1007/978-1-](https://doi.org/10.1007/978-1-4419-9905-4)
870 [4419-9905-4](https://doi.org/10.1007/978-1-4419-9905-4)

871 Dahlman, J., Sjörs, A., Lindström, J., Ledin, T., & Falkmer, T. (2009). Performance and Autonomic
872 Responses During Motion Sickness. *Human Factors: The Journal of the Human Factors and Ergonomics*
873 *Society*, 51(1), 56-66. <https://doi.org/10.1177/0018720809332848>

874 Denise, P., Vouriot, A., Normand, H., Golding, J. F., & Gresty, M. A. (2009). Effect of temporal
875 relationship between respiration and body motion on motion sickness. *Autonomic Neuroscience*, 151(2),
876 142-146. <https://doi.org/10.1016/j.autneu.2009.06.007>

877 Dennison, M. S., Wisti, A. Z., & D'Zmura, M. (2016). Use of physiological signals to predict cybersickness.
878 *Displays*, 44, 42-52. <https://doi.org/10.1016/j.displa.2016.07.002>

879 Diels, C. (2014). Will autonomous vehicles make us sick? In S. Sharples & S. Shorrock (Éds.),
880 *Contemporary Ergonomics and Human Factors 2014* (p. 301-307). Taylor & Francis.
881 <https://doi.org/10.1201/b16742-56>

882 Diels, C., & Bos, J. E. (2016). Self-driving carsickness. *Applied Ergonomics*, 53, 374-382.
883 <https://doi.org/10.1016/j.apergo.2015.09.009>

884 Donohew, B. E., & Griffin, M. J. (2004). *Motion Sickness : Effect of the Frequency of Lateral Oscillation*.
885 75(8), 8.

886 Feenstra, P. J., Bos, J. E., & van Gent, R. N. H. W. (2011). A visual display enhancing comfort by
887 counteracting airsickness. *Displays*, 32(4), 194-200. <https://doi.org/10.1016/j.displa.2010.11.002>

888 Feng, F. (2017). Can vehicle longitudinal jerk be used to identify aggressive drivers ? An examination using
889 naturalistic driving data. *Accident Analysis and Prevention*, 12.

890 Gavgani, A. M., Nesbitt, K. V., Blackmore, K. L., & Nalivaiko, E. (2017). Profiling subjective symptoms
891 and autonomic changes associated with cybersickness. *Autonomic Neuroscience*, 203, 41-50.
892 <https://doi.org/10.1016/j.autneu.2016.12.004>

893 Gianaros, P. J., Quigley, K. S., Muth, E. R., Levine, M. E., Vasko, Jr., R. C., & Stern, R. M. (2003).
894 Relationship between temporal changes in cardiac parasympathetic activity and motion sickness severity.
895 *Psychophysiology*, 40(1), 39-44. <https://doi.org/10.1111/1469-8986.00005>

896 Golding, J. F. (2006). Motion sickness susceptibility. *Autonomic Neuroscience*, 129(1-2), 67-76.
897 <https://doi.org/10.1016/j.autneu.2006.07.019>

898 Golding, J. F., Mueller, A. G., & Gresty, M. A. (2001). A motion sickness maximum around the 0.2 Hz
899 frequency range of horizontal translational oscillation. *Aviation, Space, and Environmental Medicine*,
900 72(3), Article 3.

901 Green, P. (2016). *Motion Sickness and Concerns for Self-Driving Vehicles : A Literature Review*. 83.

902 Griffin, M. J., & Newman, M. M. (2004). An experimental study of low-frequency motion in cars.
903 *Proceedings of the Institution of Mechanical Engineers, Part D: Journal of Automobile Engineering*,
904 218(11), 1231-1238. <https://doi.org/10.1243/0954407042580093>

905 Harm, D. L. (2002). *Motion Sickness Neurophysiology, Physiological Correlates, and Treatment*. 29.

906 Hendricks, R., & Tumpey, T. (1990). Contribution of virus and immune factors to herpes simplex virus
907 type I-induced corneal pathology. *Investigative ophthalmology & visual science*, 31, 1929-1939.

908 Henry, E. H., Bougard, C., Bourdin, C., & Bringoux, L. (2022). Changes in Electroencephalography
909 Activity of Sensory Areas Linked to Car Sickness in Real Driving Conditions. *Frontiers in Human*
910 *Neuroscience*, 15. <https://www.frontiersin.org/articles/10.3389/fnhum.2021.809714>

911 Himi, N., Koga, T., Nakamura, E., Kobashi, M., Yamane, M., & Tsujioka, K. (2004). Differences in
912 autonomic responses between subjects with and without nausea while watching an irregularly oscillating
913 video. *Autonomic Neuroscience*, 116(1-2), 46-53. <https://doi.org/10.1016/j.autneu.2004.08.008>

914 Hu, S., Grant, W. F., Stern, R. M., & Koch, K. L. (1991). Motion sickness severity and physiological
915 correlates during repeated exposures to a rotating optokinetic drum. *Aviation, Space, and Environmental*
916 *Medicine*, 62, 308-314.

917 Irmak, T. (2021). Objective and subjective responses to motion sickness : The group and the individual.
918 *Experimental Brain Research*, 17.

919 Islam, R., Lee, Y., Jaloli, M., Muhammad, I., Zhu, D., & Quarles, J. (2020). *Automatic Detection of*
920 *Cybersickness from Physiological Signal in a Virtual Roller Coaster Simulation*.
921 <https://doi.org/10.1109/VRW50115.2020.00175>

922 Kennedy. (1993). *Kennedy et al, 1993 Simulator sickness questionnaire : An enhanced method for*
923 *quantifying simulator sickness*.

924 Kennedy, R. S., Drexler, J., & Kennedy, R. C. (2010). Research in visually induced motion sickness.
925 *Applied Ergonomics*, 41(4), 494-503. <https://doi.org/10.1016/j.apergo.2009.11.006>

926 Keshavarz, B., Peck, K., Rezaei, S., & Taati, B. (2022). Detecting and predicting visually induced motion
927 sickness with physiological measures in combination with machine learning techniques. *International*
928 *Journal of Psychophysiology*, 176, 14-26. <https://doi.org/10.1016/j.ijpsycho.2022.03.006>

929 Kim, J., & Park, T. (2020). The Onset Threshold of Cybersickness in Constant and Accelerating Optical
930 Flow. *Applied Sciences*, 10(21), 7808. <https://doi.org/10.3390/app10217808>

931 Kim, Y. Y., Kim, H. J., Kim, E. N., Ko, H. D., & Kim, H. T. (2005). Characteristic changes in the
932 physiological components of cybersickness. *Psychophysiology*, 0(0), 050826083901001-???
933 <https://doi.org/10.1111/j.1469-8986.2005.00349.x>

- 934 Koohestani, A., Nahavandi, D., Asadi, H., Kebria, P. M., Khosravi, A., Alizadehsani, R., & Nahavandi, S.
935 (2019). A Knowledge Discovery in Motion Sickness : A Comprehensive Literature Review. *IEEE Access*,
936 7, 85755-85770. <https://doi.org/10.1109/ACCESS.2019.2922993>
- 937 Kuiper, O. X., Bos, J. E., & Diels, C. (2018). Looking forward : In-vehicle auxiliary display positioning
938 affects carsickness. *Applied Ergonomics*, 68, 169-175. <https://doi.org/10.1016/j.apergo.2017.11.002>
- 939 Kuiper, O. X., Bos, J. E., Diels, C., & Schmidt, E. A. (2020). Knowing what's coming : Anticipatory audio
940 cues can mitigate motion sickness. *Applied ergonomics*, 85, 103068.
- 941 Kuiper, O. X., Bos, J. E., Schmidt, E. A., Diels, C., & Wolter, S. (2020). Knowing What's Coming :
942 Unpredictable Motion Causes More Motion Sickness. *Human Factors: The Journal of the Human Factors*
943 *and Ergonomics Society*, 62(8), 1339-1348. <https://doi.org/10.1177/0018720819876139>
- 944 Lackner, J. R. (2014). Motion sickness : More than nausea and vomiting. *Experimental Brain Research*,
945 232(8), 2493-2510. <https://doi.org/10.1007/s00221-014-4008-8>
- 946 LaCount, L., Napadow, V., Kuo, B., Park, K., Kim, J., Brown, E., & Barbieri, R. (2009). *Dynamic*
947 *Cardiovagal Response to Motion Sickness : A Point-Process Heart Rate Variability Study*. 4.
- 948 LaCount, L. T., Barbieri, R., Park, K., Kim, J., Brown, E. N., Kuo, B., & Napadow, V. (2011). Static and
949 Dynamic Autonomic Response with Increasing Nausea Perception. *Aviation, space, and environmental*
950 *medicine*, 82(4), 424-433.
- 951 Lawther, A., & Griffin, M. J. (1987). Prediction of the incidence of motion sickness from the magnitude,
952 frequency, and duration of vertical oscillation. *J. Acoust.Soc. Am.*, 82(3), 10.
- 953 Levine, M. E., Stern, R. M., & Koch, K. L. (2014). Enhanced perceptions of control and predictability
954 reduce motion-induced nausea and gastric dysrhythmia. *Experimental brain research*, 232(8), 2675-2684.
- 955 Li, G., & Chung, W.-Y. (2013). Detection of Driver Drowsiness Using Wavelet Analysis of Heart Rate
956 Variability and a Support Vector Machine Classifier. *Sensors*, 13(12), Article 12.
957 <https://doi.org/10.3390/s131216494>
- 958 Lin, C.-T., Chuang, S.-W., Chen, Y.-C., Ko, L.-W., Liang, S.-F., & Jung, T.-P. (2007). EEG Effects of
959 Motion Sickness Induced in a Dynamic Virtual Reality Environment. *2007 29th Annual International*
960 *Conference of the IEEE Engineering in Medicine and Biology Society*, 3872-3875.
961 <https://doi.org/10.1109/IEMBS.2007.4353178>
- 962 Maculewicz, J., Larsson, P., & Fagerlönn, J. (2021). *Intuitive and subtle motion-anticipatory auditory cues*
963 *reduce motion sickness in self-driving cars*. 23.
- 964 Makowski, D. (2016). Neurokit : A python toolbox for statistics and neurophysiological signal processing
965 (eeg, eda, ecg, emg...). *Memory and Cognition Lab'Day*, 1.
- 966 Mayne. (1974). *A Systems Concept of the Vestibular Organs* | SpringerLink.
967 https://link.springer.com/chapter/10.1007/978-3-642-65920-1_14
- 968 Meteier, Q., Capallera, M., Ruffieux, S., Angelini, L., Abou Khaled, O., Mugellini, E., Widmer, M., &
969 Sonderegger, A. (2021). Classification of Drivers' Workload Using Physiological Signals in Conditional
970 Automation. *Frontiers in Psychology*, 12, 596038. <https://doi.org/10.3389/fpsyg.2021.596038>

- 971 Money, K. E. (1970). Motion sickness. *Physiological Reviews*, 50(1), 1-39.
972 <https://doi.org/10.1152/physrev.1970.50.1.1>
- 973 Mühlbacher, D., Tomzig, M., Reinmüller, K., & Rittger, L. (2020). Methodological Considerations
974 Concerning Motion Sickness Investigations during Automated Driving. *Information*, 11(5), 265.
975 <https://doi.org/10.3390/info11050265>
- 976 Muth, E. R. (2006). Motion and space sickness: Intestinal and autonomic correlates. *Autonomic
977 Neuroscience*, 129(1-2), 58-66. <https://doi.org/10.1016/j.autneu.2006.07.020>
- 978 Nalivaiko, E., Davis, S. L., Blackmore, K. L., Vakulin, A., & Nesbitt, K. V. (2015). Cybersickness
979 provoked by head-mounted display affects cutaneous vascular tone, heart rate and reaction time. *Physiology
980 & Behavior*, 151, 583-590. <https://doi.org/10.1016/j.physbeh.2015.08.043>
- 981 Napoletano, P., & Rossi, S. (2018). Combining heart and breathing rate for car driver stress recognition.
982 *2018 IEEE 8th International Conference on Consumer Electronics - Berlin (ICCE-Berlin)*, 1-5.
983 <https://doi.org/10.1109/ICCE-Berlin.2018.8576164>
- 984 Naqvi, S. A. A., Badruddin, N., Jatoi, M. A., Malik, A. S., Hazabbah, W., & Abdullah, B. (2015). EEG
985 based time and frequency dynamics analysis of visually induced motion sickness (VIMS). *Australasian
986 Physical & Engineering Sciences in Medicine*, 38(4), 721-729. <https://doi.org/10.1007/s13246-015-0379-9>
- 987 Nunan, D., Sandercock, G. R. H., & Brodie, D. A. (2010). A Quantitative Systematic Review of Normal
988 Values for Short-Term Heart Rate Variability in Healthy Adults: REVIEW OF SHORT-TERM HRV
989 VALUES. *Pacing and Clinical Electrophysiology*, 33(11), 1407-1417. [https://doi.org/10.1111/j.1540-
8159.2010.02841.x](https://doi.org/10.1111/j.1540-
990 8159.2010.02841.x)
- 991 O'Hanlon, J. F., & McCauley, M. E. (1974). Motion sickness incidence as a function of the frequency and
992 acceleration of vertical sinusoidal motion. *Aerospace Medicine*, 45(4), 366-369.
- 993 Ohyama, S., Nishiike, S., Watanabe, H., Matsuoka, K., Akizuki, H., Takeda, N., & Harada, T. (2007).
994 Autonomic responses during motion sickness induced by virtual reality. *Auris Nasus Larynx*, 34(3),
995 303-306. <https://doi.org/10.1016/j.anl.2007.01.002>
- 996 Perrin, P., Lion, A., Bosser, G., Gauchard, G., & Meistelman, C. (2013). Motion Sickness in Rally Car Co-
997 Drivers. *Aviation, Space, and Environmental Medicine*, 84(5), 473-477.
998 <https://doi.org/10.3357/ASEM.3523.2013>
- 999 Pukhova, V., Gorelova, E., Ferrini, G., & Burnasheva, S. (2017). Time-frequency representation of signals
1000 by wavelet transform. *2017 IEEE Conference of Russian Young Researchers in Electrical and Electronic
1001 Engineering (EIConRus)*, 715-718. <https://doi.org/10.1109/EIConRus.2017.7910658>
- 1002 Reason, J. T. (1978). Motion Sickness Adaptation: A Neural Mismatch Model. *Journal of the Royal Society
1003 of Medicine*, 71(11), 819-829. <https://doi.org/10.1177/014107687807101109>
- 1004 Reason, J. T., & Brand, J. J. (1975). *Motion sickness* (p. vii, 310). Academic Press.
- 1005 Rolnick, A., & Lubow, R. E. (1991). Why is the driver rarely motion sick? The role of controllability in
1006 motion sickness. *Ergonomics*, 34(7), 867-879. <https://doi.org/10.1080/00140139108964831>
- 1007 Salahuddin, L., Cho, J., Jeong, M. G., & Kim, D. (2007, August). Ultra short term analysis of heart rate
1008 variability for monitoring mental stress in mobile settings. In 2007 29th annual international conference of

1009 the ieee engineering in medicine and biology society (pp. 4656-4659). IEEE.
1010 <https://doi.org/10.1109/IEMBS.2007.4353378>

1011 Salter, S., Diels, C., Herriotts, P., Kanarachos, S., & Thake, D. (2019). Motion sickness in automated
1012 vehicles with forward and rearward facing seating orientations. *Applied Ergonomics*, 78, 54-61.
1013 <https://doi.org/10.1016/j.apergo.2019.02.001>

1014 Schmidt, E. A., Kuiper, O. X., Wolter, S., Diels, C., & Bos, J. E. (2020). An international survey on the
1015 incidence and modulating factors of carsickness. *Transportation Research Part F: Traffic Psychology and*
1016 *Behaviour*, 71, 76-87. <https://doi.org/10.1016/j.trf.2020.03.012>

1017 Sclocco, R., Kim, J., Garcia, R. G., Sheehan, J. D., Beissner, F., Bianchi, A. M., Cerutti, S., Kuo, B.,
1018 Barbieri, R., & Napadow, V. (2016). Brain Circuitry Supporting Multi-Organ Autonomic Outflow in
1019 Response to Nausea. *Cerebral Cortex*, 26(2), 485-497. <https://doi.org/10.1093/cercor/bhu172>

1020 Shaffer, F., & Ginsberg, J. P. (2017). An Overview of Heart Rate Variability Metrics and Norms. *Frontiers*
1021 *in Public Health*, 5, 258. <https://doi.org/10.3389/fpubh.2017.00258>

1022 Shoeb, A., & Clifford, G. (2005). *Chapter 16—Wavelets; Multiscale Activity in Physiological Signals*.
1023 http://www.mit.edu/~gari/teaching/6.555/LECTURE_NOTES/wavelet_lecture_notes.pdf

1024 Sivak, M., & Schoettle, B. (2015). *MOTION SICKNESS IN SELF-DRIVING VEHICLES*. 15.

1025 Smyth, J., Jennings, P., Bennett, P., & Birrell, S. (2021). A novel method for reducing motion sickness
1026 susceptibility through training visuospatial ability – A two-part study. *Applied Ergonomics*, 90, 103264.
1027 <https://doi.org/10.1016/j.apergo.2020.103264>

1028 Sweeney, M. and Bartell, E. (2017). *Sensory Stimulation System for an Autonomous Vehicle*,
1029 *US20170313326*, U.S. Patent and Trademark Office, Washington, DC.

1030 Taylor, S., Jaques, N., Chen, W., Fedor, S., Sano, A., & Picard, R. (2015). Automatic identification of
1031 artifacts in electrodermal activity data. *2015 37th Annual International Conference of the IEEE Engineering*
1032 *in Medicine and Biology Society (EMBC)*, 1934-1937. <https://doi.org/10.1109/EMBC.2015.7318762>

1033 Turner, M. (1999). Motion sickness in public road transport : Passenger behaviour and susceptibility.
1034 *Ergonomics*, 42(3), 444-461. <https://doi.org/10.1080/001401399185586>

1035 Wada, T., Fujisawa, S., & Doi, S. (2018). Analysis of driver's head tilt using a mathematical model of
1036 motion sickness. *International Journal of Industrial Ergonomics*, 63, 89-97.
1037 <https://doi.org/10.1016/j.ergon.2016.11.003>

1038 Wada, T., Konno, H., Fujisawa, S., & Doi, S. (2012). Can Passengers' Active Head Tilt Decrease the
1039 Severity of Carsickness? : Effect of Head Tilt on Severity of Motion Sickness in a Lateral Acceleration
1040 Environment. *Human Factors: The Journal of the Human Factors and Ergonomics Society*, 54(2), 226-234.
1041 <https://doi.org/10.1177/0018720812436584>

1042 Wada, T., & Yoshida, K. (2016). Effect of passengers' active head tilt and opening/closure of eyes on
1043 motion sickness in lateral acceleration environment of cars. *Ergonomics*, 59(8), 1050-1059.
1044 <https://doi.org/10.1080/00140139.2015.1109713>

1045 Wood, S. J. (2002). Human otolith-ocular reflexes during off-vertical axis rotation : Effect of frequency on
1046 tilt-translation ambiguity and motion sickness. *Neuroscience Letters*, 323(1), 41-44.
1047 [https://doi.org/10.1016/S0304-3940\(02\)00118-0](https://doi.org/10.1016/S0304-3940(02)00118-0)

1048 Yen Pik Sang, F., Golding, J. F., & Gresty, M. A. (2003). Suppression of sickness by controlled breathing
 1049 during mildly nauseogenic motion. *Aviation, Space, and Environmental Medicine*, 74(9), Article 9.

1050

1051 **7 Supplementary material**

	REGULAR LOW					UNPREDICTABLE LOW				
	Bas	S _{start}	S _{mid}	S _{stop}	Recov	Bas	S _{start}	S _{mid}	S _{stop}	Recov
CSR	0.0 ± 0.0	0.3 ± 0.1	0.8 ± 0.2	1.0 ± 0.3	0.8 ± 0.3	0.0 ± 0.0	0.5 ± 0.2	1.5 ± 0.2	2.3 ± 0.3	0.9 ± 0.3
HR_mean	77.73 ± 3.66	80.68 ± 3.11	77.97 ± 2.54	77.42 ± 2.72	73.24 ± 2.63	69.68 ± 2.18	79.20 ± 2.78	79.08 ± 3.19	80.72 ± 3.77	78.20 ± 2.98
HR_std	3.19 ± 0.37	2.94 ± 0.40	3.16 ± 0.50	2.65 ± 0.33	3.54 ± 0.58	3.17 ± 0.35	2.81 ± 0.32	3.13 ± 0.64	3.38 ± 0.61	3.02 ± 0.40
In_max	1.78 ± 0.37	2.82 ± 0.39	2.83 ± 0.41	2.95 ± 0.47	1.93 ± 0.27	2.16 ± 0.67	3.66 ± 0.68	4.13 ± 0.75	3.80 ± 0.71	2.07 ± 0.40
Out_max	1.70 ± 0.31	3.01 ± 0.48	3.07 ± 0.45	2.92 ± 0.42	1.93 ± 0.22	2.43 ± 0.63	3.82 ± 0.78	4.14 ± 0.75	3.83 ± 0.68	2.12 ± 0.46
Scr_mean	0.79 ± 0.14	1.46 ± 0.48	1.42 ± 0.40	1.78 ± 0.49	0.97 ± 0.20	0.67 ± 0.10	0.97 ± 0.16	1.06 ± 0.30	2.14 ± 0.85	0.68 ± 0.29
Scr_std	0.63 ± 0.09	1.55 ± 0.67	1.30 ± 0.46	1.42 ± 0.37	0.80 ± 0.13	0.61 ± 0.10	0.77 ± 0.11	0.90 ± 0.28	1.29 ± 0.35	0.64 ± 0.31

	REGULAR HIGH					UNPREDICTABLE HIGH				
	Bas	S _{start}	S _{mid}	S _{stop}	Recov	Bas	S _{start}	S _{mid}	S _{stop}	Recov
CSR	0.0 ± 0.0	0.4 ± 0.2	2.0 ± 0.2	3.7 ± 0.2	2.1 ± 0.3	0.0 ± 0.0	0.5 ± 0.3	2.4 ± 0.5	3.5 ± 0.3	2.1 ± 0.3
HR_mean	67.18 ± 2.80	83.12 ± 4.08	87.05 ± 6.45	84.05 ± 5.31	68.52 ± 3.76	63.89 ± 3.28	78.89 ± 5.14	80.03 ± 5.55	81.40 ± 5.84	77.89 ± 5.56
HR_std	2.66 ± 0.24	5.26 ± 1.06	4.85 ± 1.11	5.33 ± 1.07	3.01 ± 0.36	3.90 ± 1.32	9.58 ± 4.06	7.17 ± 3.97	7.53 ± 3.96	2.47 ± 0.37
In_max	4.00 ± 0.83	6.97 ± 1.04	7.01 ± 1.08	9.59 ± 1.37	6.11 ± 1.03	2.88 ± 0.75	4.81 ± 1.03	5.27 ± 1.08	5.87 ± 1.27	3.71 ± 0.71
Out_max	3.69 ± 0.63	6.95 ± 1.07	7.49 ± 1.29	10.38 ± 1.39	6.27 ± 1.08	3.05 ± 0.79	4.80 ± 1.09	5.42 ± 1.09	5.76 ± 1.18	3.99 ± 0.84
Scr_mean	0.71 ± 0.14	2.13 ± 1.07	2.81 ± 1.24	1.56 ± 0.30	0.51 ± 0.13	0.86 ± 0.25	1.01 ± 0.13	1.75 ± 0.52	1.14 ± 0.20	0.42 ± 0.09
Scr_std	0.71 ± 0.13	0.86 ± 0.13	0.96 ± 0.20	1.37 ± 0.39	0.53 ± 0.11	0.55 ± 0.16	0.90 ± 0.14	0.95 ± 0.12	0.88 ± 0.15	0.43 ± 0.11

1052 **Supplementary Table 1:** Results for each test period (Base, S_{start}, S_{mid}, S_{stop}, and Recov) in each condition (mean ±
 1053 SEM; n=23) and for each feature: mean heart rate ('Hr_mean'), standard deviation of heart rate ('Hr_std'), maximum
 1054 inspiration ('In_max') and expiration ('Out_max'), mean skin conductance response ('SCR_mean'), and standard
 1055 deviation of skin conductance response ('SCR_std').

1056

1057

1058

1059

1060

1061

1062

1063

CSR		RL					UL					RH					UH				
PATH*PERIOD*ACCEL		Bas	S_start	S_mid	S_stop	Recov	Bas	S_start	S_mid	S_stop	Recov	Bas	S_start	S_mid	S_stop	Recov	Bas	S_start	S_mid	S_stop	Recov
RL	Bas		***	***	***	***		***	***	***	***		***	***	***	***		***	***	***	***
	S_start	***		*	**	*	***		***	***	**	***		***	***	***	***		***	***	***
	S_mid	*	*				***		**	***		***		**	***	***	***		***	***	***
	S_stop	***	**				***	*	*	***		***	*	*	***	**	***	*	***	***	**
	Recov	***	*				***	**	***			***	**	***	**		***	**	***	***	**
UL	Bas		***	***	***	***		***	***	***	***		***	***	***	***		***	***	***	***
	S_start	***			*		***		***	***	*	***		***	***	***	***		***	***	***
	S_mid	***	***	**	*	**	***	***	***	***	*	***	**		***		***	*	*	***	
	S_stop	***	***	***	***	***	***	***	***	***	***	***	***		***		***	***		**	
	Recov	***	**				***	*	*	***	***	***	*	*	***	***	***	*	***	***	**
RH	Bas		***	***	***	***		***	***	***	***		***	***	***	***		***	***	***	***
	S_start	***					***		*	***		***		***	***	***	***		***	***	***
	S_mid	***	***	**	*	**	***	***			*	***	***	***	***		***	***	*	***	
	S_stop	***	***	***	***	***	***	***	***	***	***	***	***	***	***	***	***	***	***		***
	Recov	***	***	***	**	**	***	***			**	***	***		***	***	***	***		***	
UH	Bas		***	***	***	***		***	***	***	***		***	***	***	***		***	***	***	***
	S_start	***					***		*	***		***		***	***	***	***		***	***	***
	S_mid	***	***	***	***	***	***	***	*		***	***	***	*	***		***	***	***	***	
	S_stop	***	***	***	***	***	***	***	***	**	***	***	***	***		***	***	***	***	***	***
	Recov	***	***	***	**	**	***	***			**	***	***		***		***	***		***	***

1064

1065 **Supplementary Table 2:** Results of post-hoc analyses for significant interaction between 'test period', 'acceleration
1066 level', and 'path predictability' for CSR values and each test period (Base, S_start, S_mid, S_stop, and Recov) in each condition
1067 (n=23). The three independent variables are: 'ACCEL' for 'acceleration level', 'PATH' for 'path predictability', and
1068 'PERIOD' for 'test period'. Significant statistical differences between values are shown in green. *significant
1069 difference (p < 0.05), ** significant difference (p < 0.01), *** significant difference (p < 0.001).

1070

1071

HR_mean		LOW					HIGH					HR_mean		REGULAR					UNPREDICTABLE				
PERIOD*ACCEL		Bas	S_start	S_mid	S_stop	Recov	Bas	S_start	S_mid	S_stop	Recov	PATH*PERIOD		Bas	S_start	S_mid	S_stop	Recov	Bas	S_start	S_mid	S_stop	Recov
LOW	Bas		**	*	*							REG	Bas		**	***	**			*	*	**	*
	S_start	**					**						S_start	**				***	**				
	S_mid	*					*						S_mid	***				***	*				
	S_stop	*					*						S_stop	**				***	*				
	Recov						*						Recov		***	***	***	***	*	**	**	***	**
HIGH	Bas		**	*	*	*		***	***	***	***	UNPRE	Bas		***	***	***			***	***	***	***
	S_start						***				**		S_start	*				**	***				
	S_mid						***				***		S_mid	*				**	***				
	S_stop						***				***		S_stop	**				***	***				
	Recov						***	**	***	***	***		Recov	*				**	***				***

1076

1077 **Supplementary Table 3:** Results of post-hoc analyses for significant interaction between (A) 'test period' and
1078 'acceleration level' and (B) 'test period' and 'path predictability' for 'HR_mean' values and each test period (Base,
1079 S_start, S_mid, S_stop, and Recov) (n=23). The three independent variables are: 'ACCEL' for 'acceleration level', 'PATH'
1080 for 'path predictability', and 'PERIOD' for 'test period'. Significant statistical differences between values are shown
1081 in green. *significant difference (p < 0.05), ** significant difference (p < 0.01), *** significant difference (p < 0.001).

HR_std PERIOD*ACCEL	LOW					HIGH				
	Bas	S_start	S_mid	S_stop	Recov	Bas	S_start	S_mid	S_stop	Recov
LOW	Bas						*			
	S_start						*			
	S_mid						*			
	S_stop						*			
	Recov						*			
HIGH	Bas						***	*	*	
	S_start	*	*	*	*	*				***
	S_mid					*				**
	S_stop					*				**
	Recov						***	**	**	

1082

1083 **Supplementary Table 4:** Results of post-hoc analyses for significant interaction between 'test period' and
 1084 'acceleration level' for 'HR_std' values and each test period (Base, S_start, S_mid, S_stop, and Recov) (n=23). The two
 1085 independent variables are: 'ACCEL' for 'acceleration level' and 'PERIOD' for 'test period'. Significant statistical
 1086 differences between values are shown in green. * significant difference (p < 0.05), ** significant difference (p < 0.01),
 1087 *** significant difference (p < 0.001).

1088

In_max PERIOD*ACCEL	LOW					HIGH				
	Bas	S_start	S_mid	S_stop	Recov	Bas	S_start	S_mid	S_stop	Recov
LOW	Bas		*	**	*		***	***	***	**
	S_start	*			*		*	**	***	
	S_mid	**			**		*	*	***	
	S_stop	*			*		*	*	***	
	Recov		*	**	*			***	***	***
HIGH	Bas						***	***	***	**
	S_start	***	*	*	*	***			***	
	S_mid	***	**	*	*	***	***		**	*
	S_stop	***	***	***	***	***	***	***	**	***
	Recov	**				**	**		**	**

1089

1090 **Supplementary Table 5:** Results of post-hoc analyses for significant interaction between 'test period' and
 1091 'acceleration level' for 'In_max' values and each test period (Base, S_start, S_mid, S_stop, and Recov) (n=23). The two
 1092 independent variables are: 'ACCEL' for 'acceleration level' and 'PERIOD' for 'test period'. Significant statistical
 1093 differences between values are shown in green. * significant difference (p < 0.05), ** significant difference (p < 0.01),
 1094 *** significant difference (p < 0.001).

1095

1096

1097

1098

Out_max		RL					UL					RH					UH				
PATH*PERIOD*ACCEL		Bas	S_start	S_mid	S_stop	Recov	Bas	S_start	S_mid	S_stop	Recov	Bas	S_start	S_mid	S_stop	Recov	Bas	S_start	S_mid	S_stop	Recov
RL	Bas		*	*	*	.	.	***	***	***	.	.	**	***	***	**	.	*	*	**	.
	S_start	*				*	**	***	*
	S_mid	*				*	**	***	*
	S_stop	*				.	.		*		.	.	**	**	***	*
	Recov	**	***	**		.	**	**	***	**	.	.	*	*	.
UL	Bas		*	**	*	.	.	**	**	***	*	.	.	*	*	.
	S_start	***	.	.	.	**	*				**	.	*	*	***
	S_mid	***	.	.	*	***	**				***	.	.	*	***
	S_stop	***	.	.	.	**	*	.	.		**	.	*	*	***
	Recov	**	***	**		.	**	***	***	**	.	.	*	*	.
RH	Bas		***	***	***	***	.	*	**	***	.
	S_start	**	*	*	**	**	**	*	.	*	**	***				*	***	***	**	*	***
	S_mid	***	**	**	**	***	**	*	*	*	***	***				*	***	***	***	**	***
	S_stop	***	***	***	***	***	***	***	***	***	***	***	***	***		*	***	***	***	***	***
	Recov	**	*	*	*	**	*	.	.	.	**	***	.	**	***		***	**	.	.	***
UH	Bas	***	***	***	***		***	***	***	.
	S_start	*	*	***	***	***	**	***			.	.
	S_mid	*	.	.	.	*	*	.	.	.	*	**	**	***	***	.	***				***
	S_stop	**	.	.	.	*	*	.	.	.	*	***	*	**	***	.	***				***
	Recov	***	***	***	***	.	.	***	***	

1099 **Supplementary Table 6:** Results of post-hoc analyses for significant interaction between 'test period', 'acceleration
1100 level', and 'path predictability' for CSR values and each test period (Base, S_start, S_mid, S_stop, and Recov) in each condition
1101 (n=23). The three independent variables are: 'ACCEL' for 'acceleration level', 'PATH' for 'path predictability', and
1102 'PERIOD' for 'test period'. Significant statistical differences between values are shown in green. * significant
1103 difference (p < 0.05), ** significant difference (p < 0.01), *** significant difference (p < 0.001).

1104

1105

1106

SCR_mean	PERIOD					SCR_std	PERIOD				
	Bas	S_start	S_mid	S_stop	Recov		Bas	S_start	S_mid	S_stop	Recov
Bas		.	**	**	.	Bas		*	*	***	.
S_start	.		.	.	*	S_start	*		.	.	**
S_mid	**	.		.	***	S_mid	*	.		.	**
S_stop	**	.	.		**	S_stop	***	.	.		***
Recov	.	*	***	**		Recov	.	**	**	***	

1109

1110

1111 **Supplementary Table 7:** Results of post-hoc analyses for significant effect of 'test period' (A) for 'SCR_mean' and
1112 (B) for 'SCR_std' values and each test period (Base, S_start, S_mid, S_stop, and Recov) (n=23). There is one independent
1113 variable: 'PERIOD'. Significant statistical differences between values are shown in green. * significant (p
1114 < 0.05), ** significant difference (p < 0.01), *** significant difference (p < 0.001).

1115

1116